# Single-Site Anionic Polymerization. Monomeric Ester Enolaluminate Propagator Synthesis, Molecular Structure, and Polymerization Mechanism

**ARTICLE** *in* JOURNAL OF THE AMERICAN CHEMICAL SOCIETY · FEBRUARY 2005

Impact Factor: 12.11 · DOI: 10.1021/ja044671z · Source: PubMed



**2 AUTHORS:**

Antonio Rodríguez-Delgado
Universidad de Sevilla-CSIC
**28** PUBLICATIONS **562** CITATIONS
SEE PROFILE

Dajiang Liu
Colorado State University
**31** PUBLICATIONS **994** CITATIONS
SEE PROFILE

J|A|C|S
ARTICLES
Published on Web 12/24/2004

# Single-Site Anionic Polymerization. Monomeric Ester Enolaluminate Propagator Synthesis, Molecular Structure, and Polymerization Mechanism

Antonio Rodriguez-Delgado and Eugene Y.-X. Chen*

*Contribution from the Department of Chemistry, Colorado State University, Fort Collins, Colorado 80523-1872*

Received September 2, 2004; E-mail: eychen@lamar.colostate.edu

***Abstract:*** The synthesis and molecular structure of the first examples of monomeric lithium ester enolaluminates that serve as structural models for single-site anionic propagating centers, as well as the mechanism of their polymerization of methacrylates catalyzed by conjugate organoaluminum Lewis acids, are reported. Reactions of isopropyl α-lithioisobutyrate (**2**) with suitable deaggregating and stabilizing organoaluminum compounds such as $MeAl(BHT)_2$ (BHT = 2,6-di-*tert*-butyl-4-methylphenolate) in hydrocarbons cleanly generate lithium ester enolaluminate complexes such as $Li^+[Me_2C{=}C(O^iPr)OAlMe(BHT)_2]^-$ (**3**). Remarkably, complex **3** is isolable and exists as a monomer in both solid and solution states. Unlike the uncontrolled polymerization of methacrylates by the aggregating enolate **2**, the methacrylate polymerization by the monomeric **3** is controlled but exhibits low activity. However, the well controlled *and* highly active polymerization can be achieved by using the **3**/$MeAl(BHT)_2$ propagator/catalyst pair, which is conveniently generated by in situ mixing of **2** with 2 equiv of $MeAl(BHT)_2$. The structure of the added organoaluminum compounds has marked effects on the degree of monomer activation, enolaluminate formation and reactivity, and polymerization control. Kinetics of the polymerization by the **3**/$MeAl(BHT)_2$ pair suggest a bimolecular, activated-monomer anionic polymerization mechanism via single-site ester enolaluminate propagating centers. The molecular structures of activated monomer **1**, aggregated initiator **2**, and monomeric propagator **3** have been determined by X-ray diffraction studies.

## Introduction

Single-site cationic transition-metal complexes have initiated a new era in polymer synthesis, especially in the synthesis of new polyolefins.[1] In nearly a mirror-image picture, *anionic* organometallic initiators such as organolithium compounds are routinely used to polymerize polar vinyl monomers such as (meth)acrylates to technologically important functionalized vinyl polymers.[2] Organolithium compounds are the most widely used initiators in anionic polymerization reactions owing to their high versatility and reactivity toward various types of monomers; some noteworthy structural features of the common organolithium initiators include aggregation to give dimers, tetramers and higher oligomers, complexation of the Li metal center of unique size, charge density, and atomic orbitals available for bonding by solvent molecules and chelating ligands, as well as complexity and ambiguity in the nature of bonding (i.e., ionic vs covalent).[2] Specifically regarding applications of organolithium initiators in anionic polymerization of alkyl (meth)acrylates, their aggregation nature becomes a major problem of concern. Such anionic initiators as well as their derived propagating species commonly exist as aggregates, both in solid state and in solution. These anionic active species (initiators or propagators) cannot control the polymer number average molecular weight ($M_n$) and molecular weight distribution (MWD) due to the coexistence of various aggregated species that exhibit different reactivity and exchange slowly on, or comparably to, the polymerization time scale.[3] They can, however, be characterized as *multiple-site* anionic active species. Hence, an important challenge in anionic polymerization using such initiators has been the extensive and continued quests for effective additives or catalysts that can render these multiple-site anionic active species to exhibit high polymerization activities and degrees of polymerization control.[4]

Several comprehensive reviews have surveyed substantial strategies developed to achieve a high degree of polymerization control.[4] Among these strategies is a highly versatile approach that attracted the most attention: combining alkyllithium

(1) (a) Gibson, V. C.; Spitzmesser, S. K. *Chem. Rev.* **2003**, *103*, 283−315. (b) Coates, G. W.; Hustad, P. D.; Reinartz, S. *Angew. Chem., Int. Ed.* **2002**, *41*, 2236−2257. (c) Erker, G. *Acc. Chem. Res.* **2001**, *34*, 309−317. (d) Tullo, A. H. Single-Site Catalysts. *C&E News* **2000**, *Aug. 7*, 35−46. (e) Gladysz, J. A., Ed. Frontiers in Metal-Catalyzed Polymerization. *Chem. Rev.* **2000**, *100*, 1167−1682. (f) Chum, P. S.; Kruper, W. J.; Guest, M. J. *Adv. Mater.* **2000**, *12*, 1759−1767. (g) Marks, T. J., Stevens, J. C., Eds. Advances in Polymerization Catalysis. Catalysts and Processes. *Topics Catal.* **1999**, *15*, 1−208. (h) *Metalorganic Catalysts for Synthesis and Polymerization*; Kaminsky, W., Ed.; Springer: Berlin, 1999. (i) Jordan, R. F., Ed. Metallocene and Single-Site Olefin Catalysis. *J. Mol. Catal.* **1998**, *128*, 1−337. (j) Bochmann, M. *J. Chem. Soc., Dalton Trans.* **1996**, 255−270. (k) Brintzinger, H.-H.; Fischer, D.; Mülhaupt, R.; Rieger, B.; Waymouth, R. M. *Angew. Chem., Int. Ed. Engl.* **1995**, *34*, 1143−1170. (l) *Catalyst Design for Tailor-Made Polyolefins*; Soga, K., Terano, M., Eds.; Elsevier: Tokyo, 1994.

(2) Hsieh, H. L.; Quirk, R. P. *Anionic Polymerization. Principles and Practical Applications*. Marcel Dekker: New York, 1996.

(3) Litvinenko, G.; Müller, A. H. E. *Macromolecules* **1997**, *30*, 1253−1266.

initiators with common organoaluminum compounds, often added in excess. This strategy was first developed by Hatada et al.[5] for the production of highly syndiotactic ([*rr*] ≥ 90%) poly(methyl methacrylate) (PMMA) with narrow MWDs ($M_w/M_n \leq 1.19$) using a $^t$BuLi/$R_3$Al (≤1/3) combination in toluene at low temperatures (≤−78 °C). By combining $^t$BuLi with a bulky aluminum additive, bis(2,6-*tert*-butylphenoxy)methylaluminum, in a 1:5 ratio, Hatada et al.[6] also obtained heterotactic ([*mr*] = 67.8%) PMMA with a narrow MWD ($M_w/M_n = 1.14$). Ballard et al.[7] produced syndiotactic ([*rr*] ≥ 70%) PMMA with narrow MWDs ($M_w/M_n = 1.09-1.28$) in toluene at elevated temperatures (0−40 °C) using a combination of $^t$BuLi with $^i$Bu$_2$Al(BHT) (BHT = butylated hydroxytoluene, formally 2,6-di-*tert*-butyl-4-methylphenolate). Schlaad and Müller[8] reported that the steric bulk and Lewis acidity of the added alkyl aluminum compounds strongly influence the tacticity and MWD of the PMMA produced by $^t$BuLi in toluene at −78 °C; depending on the aluminum compound used, the MWD is in the range $1.2 < M_w/M_n < 7$, and the tacticity of the PMMA can change from being highly syndiotactic to atactic, heterotactic, or highly isotactic. Most recently, Hatada et al.[9] reported the living polymerization of primary alkyl acrylates using a $^t$BuLi/bis(2,6-*tert*-butylphenoxy)ethylaluminum combination. Interestingly, replacing the ethyl group at Al with the smaller methyl group drastically changed the polymerization behavior, resulting in the formation of the polymer with a broad MWD in low yield.

Lithium ester enolates should be, in principle, the ideal initiators for the polymerization of alkyl (meth)acrylates because the propagating centers (**A**) for the anionic polymerization of (meth)acrylates initiated by organolithium compounds are the lithium ester enolates.[4] Rates of initiation and propagation should

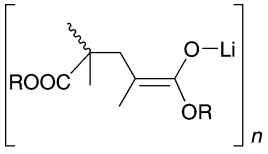


**A**

be essentially the same for such initiators, and therefore polymers with narrow MWDs should be formed. However, the lithium ester enolate propagator **A** tends to stabilize through aggregation ($n = 2-6$), and the existence of various aggregated ester enolates creates significant problems in controlling the polymerization rate and the polymer MWD.[10] Additionally,

***Scheme 1***

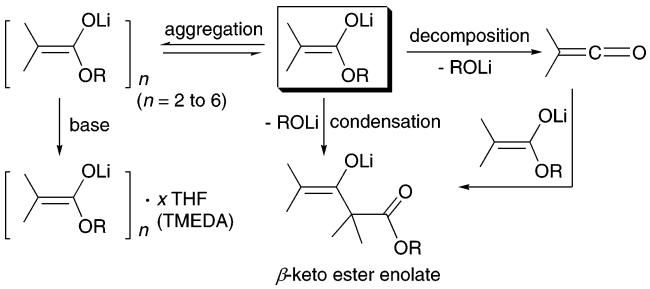


lithium ester enolates are unstable, even in the solid state, and subject to decomposition to ketenes and lithium alkoxides and β-keto ester enolates.[11] Lithium ester enolates have a strong tendency to aggregate in both crystalline[12] and solution[13] states, which affect their reactivity as initiators and the resulting polymer MWD. Scheme 1 summaries the above-mentioned complexity and instability of typical lithium ester enolates. As a result, anionic polymerizations by lithium ester enolates in nonpolar solvents proceed largely in an uncontrolled manner, leading to polymers with broad or multimodal MWDs.[14] Again, this uncontrolled polymerization behavior is attributed to the coexistence of multiple active sites, which exhibit different reactivity and exchange slowly on the polymerization time scale, and to the side reactions of ester enolate propagating species.

A strategy to overcome the aggregation and side reaction problems associated with lithium *ester enolate* initiators is the same as that employed for the lithium *alkyl* initiators, that is, combining the initiator with organoaluminum alkyls. Schlaad and Müller[15] proposed, on the basis of the $^{13}$C NMR spectroscopic evidence, that the bimetallic "ate" complex (**B**) is an adequate model of the active center for the MMA polymerization by ethyl α-lithioisobutyrate (EiBLi) in the presence of aluminum alkyls. Complex **B** was detectable by $^{13}$C NMR up to 0 °C; at

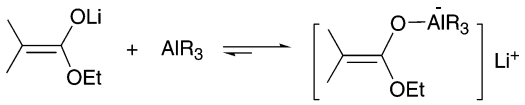


EiBLi **B**

ambient temperature, irreversible decomposition takes place. The calculated structures for the complex of methyl α-lithioisobutyrate (MiBLi) with $AlEt_3$, however, reveal different degrees of association, $(MiBLi{\cdot}AlEt_3)_n$ ($n$ = 1, 2, 4), and different stoichiometries, MiBLi·$x$AlEt$_3$ ($x$ = 1, 2).[16] We found that the addition of 2 equiv of the strongly Lewis acidic alane, $Al(C_6F_5)_3$, to the otherwise uncontrolled MMA polymerization by MiBLi,

(4) For comprehensive reviews, see: (a) Baskaran, D. *Prog. Polym. Sci.* **2003**, *28*, 521−5811. (b) Vlček, P.; Lochmann, L. *Prog. Polym. Sci.* **1999**, *24*, 793−973. (c) Zune, C.; Jérôme, R. *Prog. Polym. Sci.* **1999**, *24*, 631−664. (d) Hatada, K.; Kitayama, T.; Ute, K. *Prog. Polym. Sci.* **1988**, *13*, 189−276. (e) Van Beylen, M.; Bywater, S.; Smets, G.; Szwarc, M.; Worsfold, D. J. *Adv. Polym. Sci.* **1988**, *86*, 87−143.
(5) (a) Kitayama, T.; Shinozaki, T.; Sakamoto, T.; Yamamoto, M.; Hatada, K. *Makromol. Chem. Suppl.* **1989**, *15*, 167−185. (b) Kitayama, T.; Shinozaki, T.; Masuda, E.; Yamamoto, M.; Hatada, K. *Polym. Bull.* **1988**, *20*, 505−510.
(6) (a) Kitayama, T.; Hirano, T.; Hatada, K. *Tetrahedron* **1997**, *53*, 15263−15279. (b) Kitayama, T.; Hirano, T.; Zhang, Y.; Hatada, K. *Macromol. Symp.* **1996**, *107*, 297−306. (c) Hatada, K.; Kitayama, T.; Ute, K.; Nishiura, T. *Macromol. Symp.* **1995**, *89*, 465−478.
(7) Ballard, D. G. H.; Bowles, R. J.; Haddleton, D. M.; Richards, S. N.; Sellens, R.; Twose, D. L. *Macromolecules* **1992**, *25*, 5907−5913.
(8) Schlaad, H.; Müller, A. H. E. *Macromol. Symp.* **1996**, *107*, 163−176.
(9) Tabuchi, M.; Kawauchi, T.; Kitayama, T.; Hatada, K. *Polymer* **2002**, *43*, 7185−7190.
(10) Kunkel, D.; Müller, A. H. E.; Janata, M.; Lochmann, L. *Macromol. Symp.* **1992**, *60*, 315−326.
(11) Seebach, D. *Angew. Chem., Int. Engl.* **1988**, *27*, 1624−1654.
(12) Seebach, D.; Amstutz, R.; Laube, T.; Schweizer, W. B.; Dunitz, J. D. *J. Am. Chem. Soc.* **1985**, *107*, 5403−5409.
(13) (a) Yakimansky, A. V.; Müller, A. H. E. *J. Am. Chem. Soc.* **2001**, *123*, 4932−4937. (b) Yakimansky, A. V.; Müller, A. H. E. *Macromolecules* **1999**, *32*, 1731−1736. (c) Weiss, H.; Yakimansky, A. V.; Müller, A. H. E. *J. Am. Chem. Soc.* **1996**, *118*, 8897−8903. (d) Kříž, J.; Dybal, J.; Vlček, P.; Janata, M. *Macromol. Chem. Phys.* **1994**, *195*, 3039−3056. (e) Wang, J. S.; Jérôme, R.; Warin, R.; Teyssié, Ph. *Macromolecules* **1993**, *26*, 1402−1406. (f) Halaska, V.; Lochmann, L. *Collect. Czech. Chem. Commun.* **1973**, *38*, 1780−1782.
(14) (a) Bolig, A. D.; Chen, E. Y.-X. *J. Am. Chem. Soc.* **2001**, *123*, 7943−7944. (b) Schmitt, B.; Schlaad, H.; Müller, A. H. E. *Macromolecules* **1998**, *31*, 1705−1709.
(15) (a) Schlaad, H.; Müller, A. H. E. *Macromol. Symp.* **1995**, *95*, 13−26. (b) Schlaad, H.; Müller, A. H. E. *Macromol. Rapid. Commun.* **1994**, *15*, 517−525.
(16) Schmitt, B.; Schlaad, H.; Müller, A. H. E.; Mathiasch, B.; Steiger, S.; Weiss, H. *Macromolecules* **1999**, *32*, 8340−8349.

1 equiv for generating the lithium ester enolaluminate propagating species and the other for activating monomer, brings about a much faster and more controlled polymerization than that by MiBLi alone, producing syndiotactic PMMA with [*rr*] ranging from moderate 78% to high 94%, glass-transition temperatures ($T_g$) from 127 to 138 °C, and MWDs as narrow as 1.08, depending on polymerization temperature.[14a] A control run using MiBLi alone in toluene at ambient temperature produced isotactic ([*mm*] = 67%) PMMA with a broad MWD ($M_w/M_n$ = 18.8) and low polymerization activity. Holmes et al.[17] investigated ligand effects of organoaluminum amides $^i\mathrm{Bu}_x\mathrm{Al(NRR')}_{3-x}$ ($x$ = 1, 2) and organoaluminum alkoxides $^i\mathrm{Bu}_x\mathrm{Al(OR)}_{3-x}$ ($x$ = 1−3) in the MMA polymerization initiated by EiBLi on polymer tacticity and MWD; they concluded that both formations of the "ate" complex (**B**-type structure) and monomer−organoaluminum complex are required to promote the controlled syndioselective polymerization. Other additives used for the lithium ester enolate-initiated (meth)acrylate polymerization, which have been shown to promote moderate to high degrees of polymerization control, include lithium *tert*-butoxide,[18] Lewis bases,[14b,19] and tetraalkylammonium (or cesium) halide−trialkylaluminum complexes.[20]

Thus, extensive research has been conducted on the strategies for achieving living and/or controlled anionic polymerization of (meth)acrylates using organolithium initiators; however, to the best of our knowledge, monomeric anionic active species (initiators and propagators) have not been unequivocally established. Inspired by the above-overviewed work of many research groups in the area of anionic polymerization of (meth)-acrylates and by the tremendous success that the single-site cationic transition-metal catalysts or initiators have achieved in the area of olefin polymerization, we sought to establish the *single-site anionic polymerization* for achieving a high degree of polymerization control. To achieve this central objective of the present study, we reasoned that, if single, uniform active species in the form of monomeric ester enolaluminate complexes, which model the structure of the active propagating species **B**, can be generated, structurally characterized, and employed to successfully control the polymerization, then the "single-site active species" concept can also be realized in anionic polymerizations by organolithium compounds. To this end, we report here the synthesis and structural characterization of the unprecedented monomeric lithium ester enolaluminates as well as their use as single-site, anionic active species in the polymerization of methacrylates. More specifically, the reactions of lithium ester enolate aggregates with suitable deaggregating and stabilizing organoaluminum compounds produce monomeric lithium ester enolaluminate active species, the structures of which have been characterized by spectroscopic, analytical, and single-crystal X-ray diffraction studies. These active species promote the rapid anionic polymerization of methacrylates with a high degree of control, and the results of the polymerization kinetics indicate a bimolecular, activated-monomer anionic polymerization mechanism through the monomeric ester enolaluminate propagating center.

## Experimental Section

**Materials and Methods.** All syntheses and manipulations of air- and moisture-sensitive materials were carried out in flamed Schlenk-type glassware on a dual-manifold Schlenk line, a high vacuum line (typically $10^{-5}$ to $10^{-7}$ Torr), or in an argon-filled glovebox (typically <1.0 ppm oxygen and moisture). NMR-scale reactions (typically in a 0.02 mmol scale) were conducted in Teflon-valve-sealed J. Young-type NMR tubes. HPLC grade organic solvents were first saturated with nitrogen during filling the solvent reservoir and then dried by passage through activated alumina (for diethyl ether, THF, and methylene chloride) followed by passage through Q-5-supported copper catalyst (for toluene and hexanes) stainless steel columns. Benzene-$d_6$, toluene-$d_8$, and THF-$d_8$ were dried over sodium/potassium alloy and vacuum-distilled or filtered, whereas $CD_2Cl_2$ and $CDCl_3$ were dried over activated Davison 4-Å molecular sieves. NMR spectra were recorded on either a Varian Inova 300 (FT 300 MHz, $^1$H; 75 MHz, $^{13}$C; 282 MHz, $^{19}$F; 44 MHz, $^6$Li) or a Varian Inova 400 spectrometer. Chemical shifts for $^1$H and $^{13}$C spectra were referenced to internal solvent resonances and are reported as parts per million relative to tetramethylsilane, whereas $^{19}$F NMR and $^6$Li NMR spectra were referenced to external $CFCl_3$ and LiCl in THF. Elemental analyses were performed by Desert Analytics, Tucson, Arizona.

Isobutyric acid, thionyl chloride, *n*-BuLi (1.6 M in hexanes), MeMgBr (3.0 M in diethyl ether), diisopropylamine, triethylamine, and 2,6-di-*tert*-butyl-4-methylphenol (butylated hydroxytoluene, BHT-H) were purchased from Aldrich Chemical Co. and used as received, except for the amines, which were degassed, dried over $CaH_2$ overnight, and then vacuum-distilled before use, and for BHT-H, which was recrystallized from hexanes prior to use. Trimethylaluminum, triisobutylaluminum, and tri(*n*-octyl)aluminum were purchased from Strem Chemical Co.

Methyl methacrylate (MMA) and *n*-butyl methacrylate (BMA) were purchased from Aldrich Chemical Co.; both monomers were first degassed and dried over $CaH_2$ overnight, followed by vacuum distillation. Final purification involved titration with neat tri(*n*-octyl)-aluminum to a yellow end point[21] followed by distillation under reduced pressure. The purified monomers were stored in a −30 °C freezer inside the glovebox.

Tris(pentafluorophenyl)borane, $B(C_6F_5)_3$, was obtained as a research gift from Boulder Scientific Co. and further purified by recrystallization from hexanes at −30 °C. Tris(pentafluorophenyl)alane, $Al(C_6F_5)_3$, as a 0.5·toluene adduct based on the elemental analysis for the vacuum-dried sample, was prepared from the exchange reaction of $B(C_6F_5)_3$ and $AlMe_3$ in a 1:3 toluene/hexanes solvent mixture in quantitative yield according to a literature procedure,[22] which is the modified synthesis of the alane first disclosed by Biagini et al.[23] *Extra caution should be exercised when handling this material because of its thermal and shock sensitivity*. Neutral organoaluminum compounds used for the generation of the lithium ester enolaluminate complexes and as catalysts for activating the monomer in polymerization, including $MeAl(BHT)_2$,[24] $^i\mathrm{BuAl(BHT)_2}$,[24] $ClAl(BHT)_2$,[25] $^i\mathrm{Bu_2Al(BHT)}$,[26] and $Al(BHT)_3$,[27] were prepared according to literature procedures.

(17) (a) Péron, G. L. N.; Peace, R. J.; Holmes, A. B. *J. Mater. Chem.* **2001**, *11*, 2915−2918. (b) Peace, R. J.; Horton, M. J.; Péron, G. L. N.; Holmes, A. B. *Macromolecules* **2001**, *34*, 8409−8411.
(18) (a) Vlček, P.; Otoupalová, J.; Janata, M.; Látalová, P.; Kurková, D.; Toman, L.; Masař, B. *Macromolecules* **2004**, *37*, 344−351. (b) Lochmann, L.; Rodová, M.; Trekoval, J. *J. Polym. Sci., Part A: Polym. Chem.* **1974**, *12*, 2091−2094.
(19) Schlaad, H.; Schmitt, B.; Müller, A. H. E.; Jüngling, S.; Weiss, H. *Macromolecules* **1998**, *31*, 573−577.
(20) (a) Schmitt, B.; Müller, A. H. E. *Macromolecules* **2001**, *34*, 2115−2120. (b) Schmitt, B.; Stauf, W.; Müller, A. H. E. *Macromolecules* **2001**, *34*, 1551−1557. (c) Schmitt, B.; Schlaad, H.; Müller, A. H. E.; Mathiasch, B.; Steiger, S.; Weiss, H. *Macromolecules* **2000**, *33*, 2887−2893. (d) Schlaad, H.; Müller, A. H. E. *Macromolecules* **1998**, *31*, 7127−7132. (e) Schlaad, H.; Schmitt, B.; Müller, A. H. E. *Angew. Chem., Int. Ed.* **1998**, *37*, 1389−1391.
(21) Allen, R. D.; Long, T. E.; McGrath, J. E. *Polym. Bull.* **1986**, *15*, 127−134.
(22) Feng, S.; Roof, G. R.; Chen, E. Y.-X. *Organometallics* **2002**, *21*, 832−839.
(23) (a) Biagini, P.; Lugli, G.; Abis, L.; Andreussi, P. U.S. Pat. 5,602,269, 1997. (b) Lee, C. H.; Lee, S. J.; Park, J. W.; Kim, K. H.; Lee, B. Y.; Oh, J. S. *J. Mol. Catal., A: Chem.* **1998**, *132*, 231−239.
(24) Shreve, A. P.; Mulhaupt, R.; Fultz, W.; Calabrese, J.; Robbins, W.; Ittel, S. *Organometallics* **1988**, *7*, 409−416.

**Preparation of MMA·Al($C_6F_5$)$_3$ (1).** The activated monomer adduct **1**[14a] was prepared by adding MMA to a toluene solution of the alane, followed by removal of the volatiles in vacuo. Single crystals of **1** suitable for X-ray diffraction were grown from hexanes at −30 °C in a freezer inside the glovebox.

$^1$H NMR ($C_6D_6$, 23 °C): $\delta$ 5.80 and 4.92 (m, 1H each, C$H_2$═), 3.05 (s, 3H, −OC$H_3$), 1.22 (s, 3H, −C$H_3$). $^{19}$F NMR ($C_6D_6$, 23 °C): $\delta$ −123.38 (dd, 6F, *o*-F), −151.60 (t, 3F, *p*-F), −160.83 (m, 6F, *m*-F). $^{13}$C NMR ($C_6D_6$, 23 °C): $\delta$ 176.70 (C═O), 136.35 (*C*H$_2$═), 133.01 [*C*(Me)═], 57.18 (O*C*H$_3$), 16.64 (*C*H$_3$). (Carbons for the $C_6F_5$ groups omitted because of C−F coupling.)

**Preparation of Me$_2$C═C(O$^i$Pr)OLi (2).** The precursor isopropyl isobutyrate was prepared from the reaction of isobutyryl chloride and dry 2-propanol in diethyl ether at room temperature, in the presence of triethylamine, followed by a standard extractive workup and fractional distillation. Literature procedures for the formation of *tert*-butyl α-lithioisobutyrates[28] were slightly modified to prepare isopropyl α-lithioisobutyrate **2**. The isolated lithium ester enolate was stored in a freezer at −30 °C inside the glovebox; single crystals of **2** suitable for X-ray diffraction were grown from hexanes at −30 °C inside the glovebox.

$^1$H NMR ($C_6D_6$, 23 °C) for **2**: $\delta$ 4.28 (sept, 1H, −OC*H*Me$_2$), 1.86 (s, 3H, ═C*Me*$_2$), 1.76 (s, 3H, ═C*Me*$_2$), 1.24 (d, 6H, −CH*Me*$_2$). $^{13}$C NMR ($C_6D_6$, 23 °C): $\delta$ 156.15 (O*C*(O$^i$Pr)═), 78.01 (═*C*Me$_2$), 72.21 (O*C*HMe$_2$), 22.27 (OCH*Me*$_2$), 18.07 (═C*Me*$_2$), 17.71 (═C*Me*$_2$).

**Synthesis of Li$^+$[Me$_2$C═C(O$^i$Pr)OAlMe(BHT)$_2$]$^-$ (3).** In an argon-filled glovebox, a 30-mL glass reactor was equipped with a magnetic stir bar and charged with 0.19 g (0.46 mmol) of MeAl(BHT)$_2$ in 10 mL of toluene. To this solution, with vigorous stirring at ambient temperature, was added a solution of **2** (0.08 g, 0.58 mmol) in 10 mL of toluene in one portion. The resulting clear solution turned to yellow immediately, and the clear yellow solution gradually became a white suspension after being stirred for 30 min. Stirring was continued for an additional 30 min at ambient temperature, after which the solvent was removed in vacuo. The solid residue was extracted with 3 × 5 mL hexanes; the extract was filtered through a pad of Celite, and the light yellow filtrate was concentrated to one-half of its volume. The concentrated filtrate was left inside a freezer at −30 °C, yielding 0.20 g (80%) of the pure product as a colorless microcrystalline solid after filtration and drying in vacuo. Single crystals suitable for X-ray diffraction analysis were obtained by slow recrystallization from toluene layered with hexanes at −30 °C inside a freezer of the glovebox.

$^1$H NMR ($C_6D_6$, 23 °C) for **3**: $\delta$ 7.17 (s, 4H, Ar), 3.95 (sept, 1H, −OC*H*Me$_2$), 2.25 (s, 6H, Ar−C$H_3$), 1.87 (s, 3H, ═C*Me*$_2$), 1.54 (s, 3H, ═C*Me*$_2$), 1.49 (s, 36H, Ar−C*Me*$_3$), 0.78 (d, 6H, −CH*Me*$_2$), 0.11 (s, 3H, Al−*Me*). $^{13}$C NMR ($C_6D_6$, 23 °C): $\delta$ 154.14 (O−*C*$_{ipso}$, BHT), 150.55 [O*C*(O$^i$Pr)═], 139.56 (*p*-*C*H, BHT), 126.50 (*m*-*C*H, BHT), 126.28 (*o*-*C*H, BHT), 87.59 (═*C*Me$_2$), 74.99 (O*C*HMe$_2$), 35.39 (*C*H$_3$, BHT), 31.99 (C*Me*$_3$, BHT), 22.15 (OCH*Me*$_2$), 21.10 (*C*Me$_3$, BHT), 18.63 (═C*Me*$_2$), 17.45 (═C*Me*$_2$), −3.97 (Al*Me*). $^6$Li NMR ($C_6D_6$, 23 °C): $\delta$ −1.00. Anal. Calcd for $C_{38}H_{62}AlLiO_4$: C, 73.99; H, 10.13. Found: C, 73.28; H, 9.75.

**Synthesis of Li$^+$[Me$_2$C═C(O$^i$Pr)OAl($^i$Bu)$_3$]$^-$ (4).** The reaction of **2** and Al($^i$Bu)$_3$ was carried out in the same manner as for the synthesis of **3** shown above, affording **4** (82%) as a colorless oil. The isolated, spectroscopically pure **4** remained as an oily product after repeated crystallization attempts in hexanes at low temperatures.

$^1$H NMR ($C_6D_6$, 23 °C) for **4**: $\delta$ 4.37 (sept, 1H, −OC*H*Me$_2$), 2.09 (sept, 3H, −CH$_2$C*H*Me$_2$), 1.61 (s, 3H, ═CMe$_2$), 1.44 (s, 3H, ═CMe$_2$), 1.21 (d, $J$ = 6.3 Hz, 18H, −CH$_2$CH*Me*$_2$), 1.07 (b, 6H, −OCH*Me*$_2$), 0.07 (d, $J$ = 6.9 Hz, 6H, −C*H*$_2$CHMe$_2$). $^{13}$C NMR ($C_6D_6$, 23 °C): $\delta$ 147.95 [O*C*(O$^i$Pr)═], 92.02 (═*C*Me$_2$), 74.05 (O*C*HMe$_2$), 28.93 (CH$_2$-CH*Me*$_2$), 26.05 (CH$_2$*C*HMe$_2$), 25.04 (*C*H$_2$CHMe$_2$), 22.15 (OCH*Me*$_2$), 18.51(═C*Me*$_2$), 17.46 (═C*Me*$_2$). Anal. Calcd for $C_{19}H_{40}AlLiO_2$: C, 68.22; H, 12.07. Found: C, 67.36; H, 11.51.

**Synthesis of Li$^+$(THF)$_2$[Me$_2$C═C(O$^i$Pr)OAl($C_6F_5$)$_3$]$^-$ (5).** In an argon-filled glovebox, a 20-mL glass reactor was equipped with a magnetic stir bar and charged with 0.1 g (0.17 mmol) of Al($C_6F_5$)$_3$·0.5 toluene in 5 mL of toluene. To this reactor, with vigorous stirring at ambient temperature, was added a solution of **2** (0.024 g, 0.17 mmol) in 5 mL of toluene and 0.2 mL of THF. After being stirred at ambient temperature for 15 min, the resultant light-yellow clear solution was evacuated to dryness. The yellow oily residue was extracted with 3 × 3 mL of hexanes; the extract was filtered, and the light yellow filtrate was concentrated to one-half of its volume. The concentrated filtrate was left inside a freezer at −30 °C for several hours, yielding 0.084 g (61%) of the spectroscopically pure product as a colorless microcrystalline solid after filtration and drying in vacuo. This complex is thermally unstable, and several attempts to obtain single crystals suitable for X-ray diffraction analysis were unsuccessful.

$^1$H NMR ($C_6D_6$, 23 °C) for **5**: $\delta$ 4.12 (sept, 1H, −OC*H*Me$_2$), 3.30 (m, 8H, α-C$H_2$, THF), 1.61 (s, 3H, ═C*Me*$_2$), 1.43 (s, 3H, ═C*Me*$_2$), 1.22 (m, 8H, *β*-C$H_2$, THF), 0.89 (d, $J$ = 6.0 Hz, 6H, −CH*Me*$_2$). $^{13}$C NMR ($C_6D_6$, 23 °C): $\delta$ 151.80 [O*C*(O$^i$Pr)═], 148.85, 142.96, 138.66, 135.39 (*C*$_6$F$_5$), 92.01 (═*C*Me$_2$), 71.93 (O*C*HMe$_2$), 68.45 (α-*C*H$_2$, THF), 25.45 (*β*-*C*H$_2$, THF), 21.47 (OCH*Me*$_2$), 20.82 (═C*Me*$_2$), 17.83 (═C*Me*$_2$). $^{19}$F NMR ($C_6D_6$, 23 °C): $\delta$ −124.89 (d, $^3J_{F-F}$ = 19.5 Hz, 6F, *o*-F), −154.20 (t, $^3J_{F-F}$ = 20.9 Hz, 3F, *p*-F), −161.76 (m, 6F, *m*-F).

**X-ray Crystallographic Analyses of 1, 2, and 3.** Single crystals suitable for X-ray diffraction studies were quickly covered with a layer of Paratone-N oil (Exxon, dried and degassed at 120 °C/10$^{-6}$ Torr for 24 h) after decanting the mother liquors in the glovebox. The crystals were then mounted on thin glass fibers and transferred into the cold nitrogen steam of a Siemens SMART CCD diffractometer. The structures were solved by direct methods and refined using the Siemens SHELXTL program library.[29] The structures were refined by full-matrix-weighted least-squares on $F^2$ for all reflections. All non-hydrogen atoms were refined with anisotropic displacement parameters, whereas hydrogen atoms were included in the structure factor calculations at idealized positions. In **2**, there is a hexane molecule in the lattice, and half of the molecule is unique and present in the asymmetric unit due to a crystallographically imposed inversion center. Selected crystal data and structural refinement parameters are collected in Table 1.

**Polymerization Procedures and Polymer Characterizations.** Polymerizations were performed either in 30-mL, oven- and flame-dried vacuum flasks inside the glovebox for ambient-temperature reactions or in 25-mL oven- and flame-dried Schlenk flasks interfaced to the dual-manifold Schlenk line for lower temperature reactions. In a typical procedure, a 2.5-mL stock solution of MeAl(BHT)$_2$ (93.4 $\mu$mol) was mixed in a flask with a solution of the lithium ester enolate **2** in 2.5 mL of toluene (46.7 $\mu$mol) and stirred for 10 min to cleanly generate the initiator/catalyst pair, **3**/MeAl(BHT)$_2$. MMA (1.00 mL, 9.35 mmol) or BMA (1.48 mL, 9.35 mmol) was quickly added via pipette (for polymerizations in the glovebox) or gastight syringe (for polymerizations on the Schlenk line), and the flask was sealed and kept under vigorous stirring at the desired temperature. For block copolymerizations, a second quantity of MMA or BMA was added after the completion of the first block (1 h), and the polymerization was continued. After the measured time interval, the polymerization was quenched by the addition of 5 mL of 5% HCl-acidified methanol.

(25) Healy, M. D.; Ziller, J. W.; Barron, A. R. *Organometallics* **1992**, *11*, 3041−3049.
(26) (a) Skowronska-Ptasinska, M.; Starowieyski, K. B.; Pasynkiewicz, S.; Carewska, M. *J. Organomet. Chem.* **1978**, *160*, 403−409. (b) Starowieyski, K. B.; Pasynkiewicz, S.; Skowronska-Ptasinska, M. *J. Organomet. Chem.* **1975**, *90*, C43−C44.
(27) Healy, M. D.; Barron, A. R. *Angew. Chem., Int. Ed. Engl.* **1992**, *31*, 921−922.
(28) Kim, Y.-J.; Bernstein, M. P.; Galiano Roth, A. S.; Romesberg, F. E.; Williard, P. G.; Fuller, D. J.; Harrison, A. T.; Collum, D. B. *J. Org. Chem.* **1991**, *56*, 4435−4439.
(29) *SHELXTL*, version 6.12; Bruker Analytical X-ray Solutions: Madison, WI, 2001.

***Table 1.*** Crystal Data and Structure Refinements for **1**, [**2**]$_3$·0.5 Hexane, and **3**

| | **1** | [**2**]$_3$·0.5 hexane | **3** |
|---|---|---|---|
| empirical formula | $C_{23}H_8AlF_{15}O_2$ | $C_{24}H_{46}Li_3O_6$ | $C_{38}H_{62}AlLiO_4$ |
| formula weight | 628.27 | 451.43 | 616.80 |
| temperature/K | 173(2) | 169(2) | 173(2) |
| wavelength/Å | 0.710 73 | 0.710 73 | 0.710 73 |
| crystal system | orthorhombic | triclinic | monoclinic |
| space group | *Pbca* | $P\bar{1}$ | $P2_1/n$ |
| *a*/Å | 18.284(14) | 11.939(3) | 9.119(7) |
| *b*/Å | 12.623(10) | 12.033(3) | 24.277(17) |
| *c*/Å | 20.466(16) | 12.538(3) | 17.121(12) |
| α/deg | 90 | 72.016(4) | 90 |
| *β*/deg | 90 | 61.720(4) | 93.528(16) |
| *γ*/deg | 90 | 67.790(4) | 90 |
| volume/Å$^3$ | 4723(6) | 1449.9(6) | 3783(5) |
| *Z* | 8 | 2 | 4 |
| density (calcd)/mg/m$^3$ | 1.767 | 1.034 | 1.083 |
| abs coeff/mm$^{-1}$ | 0.226 | 0.070 | 0.088 |
| *F*(000) | 2480 | 494 | 1352 |
| crystal size/mm$^3$ | 0.10 × 0.20 × 0.30 | 0.42 × 0.38 × 0.35 | 0.38 × 0.38 × 0.10 |
| *θ* range for data collection/deg | 1.99 to 23.33 | 1.85 to 20.81 | 2.06 to 20.81 |
| index ranges | $-20 \le h \le 17$, $-14 \le k \le 13$, $-22 \le l \le 22$ | $-11 \le h \le 11$, $-12 \le k \le 12$, $-12 \le l \le 12$ | $-9 \le h \le 9$, $-24 \le k \le 24$, $-17 \le l \le 17$ |
| reflections collected | 20837 | 7300 | 18883 |
| independent reflections | 3416 [$R_{int} = 0.0809$] | 3027 [$R_{int} = 0.0532$] | 3955 [$R_{int} = 0.1117$] |
| data/restraints/parameters | 3416/0/370 | 3027/0/284 | 3955/0/398 |
| final *R* indices [$I > 2\sigma(I)$] | $R_1 = 0.0344$, $wR_2 = 0.0812$ | $R_1 = 0.0695$, $wR_2 = 0.1877$ | $R_1 = 0.0631$, $wR_2 = 0.1522$ |
| *R* indices (all data) | $R_1 = 0.0636$, $wR_2 = 0.0908$ | $R_1 = 0.0864$, $wR_2 = 0.2018$ | $R_1 = 0.0979$, $wR_2 = 0.1695$ |
| extinction coefficient | | 0.073(9) | 0.0055(10) |
| largest diff. peak and hole/eÅ$^{-3}$ | 0.289 and −0.224 | 0.442 and −0.378 | 0.272 and −0.268 |

The quenched mixture was precipitated into 100 mL of methanol, stirred for 1 h, filtered, washed with methanol, and dried in a vacuum oven at 50 °C overnight to a constant weight.

Polymer molecular weights and molecular weight distributions were measured by gel permeation chromatography (GPC) analyses carried out at 40 °C, at a flow rate of 1.0 mL/min and with THF as the eluent, on a Waters University 1500 GPC instrument. The instrument was calibrated with 10 PMMA standards, and chromatograms were processed with Waters Empower software. $^1$H NMR spectra for the analysis of PMMA and PBMA microstructures were recorded in $CDCl_3$ and analyzed according to the literature.[30]

**Polymerization Kinetics.** As control experiments, the polymerizations were first monitored by NMR-scale reactions. Stock solutions of MeAl(BHT)$_2$ (20 mM) and **2** (10 mM) in toluene-$d_8$ were prepared in the glovebox. In a typical procedure, a small vial was charged with 0.4 mL of MeAl(BHT)$_2$, 0.4 mL of **2**, and 86 $\mu$L of MMA [MMA/MeAl(BHT)$_2$/**2** = 200:2:1], and the time was recorded immediately after MMA was added to the solution mixture. The reaction mixture was subsequently loaded into a J.-Young NMR tube and transferred to an NMR spectrometer that was previously parametrized using MMA in toluene-$d_8$, for data collection.

Data were acquired at 22 °C using one scan per time interval. The ratio of [MMA]$_0$ to [MMA]$_t$ at a given time *t*, [M]$_0$/[M]$_t$, was determined by integration of the peaks for MMA (5.2 and 6.1 ppm for the vinyl signals; 3.4 ppm for the OMe signal) and PMMA (centered at 3.4 ppm for the OMe signals) according to $[M]_0/[M]_t = 2\mathbf{A}_{3.4}/3\mathbf{A}_{5.2+6.1}$, where $\mathbf{A}_{3.4}$ is the total integrals for the peaks centered at 3.4 ppm (typically in the region 3.2−3.6 ppm) and $\mathbf{A}_{5.2+6.1}$ is the total integrals for both peaks at 5.2 and 6.1 ppm. Apparent rate constants ($k_{app}$) were extracted by linearly fitting a line to the plot of $\ln([M]_0/[M]_t)$ vs time.

Kinetic experiments were also carried out in stirred Schlenk flasks using the same procedure as already described for the polymerization, except that, at appropriate time intervals, 0.2 mL aliquots were removed from the reaction mixture using syringe and quenched into 1 mL vials containing 0.6 mL of undried "wet" $CDCl_3$ mixed with 250 ppm of BHT-H. The quenched aliquots were analyzed by $^1$H NMR for determining the [M]$_0$/[M]$_t$ ratio using the same procedure as described above.

***Scheme 2***

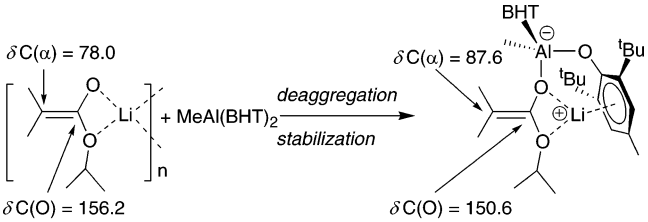


## Results and Discussion

**Synthesis of Monomeric Lithium Ester Enolaluminate Complexes.** The reaction of isopropyl α-lithioisobutyrate [$Me_2C{=}C(O^iPr)OLi$, **2**] with MeAl(BHT)$_2$ in hexanes or toluene cleanly produces the first example of an isolable lithium ester enolaluminate complex, $Li^+[Me_2C{=}C(O^iPr)OAlMe(BHT)_2]^-$ (**3**), Scheme 2. Significantly, complex **3** is stable at ambient temperature under an inert atmosphere and has been isolated as a crystalline solid; the single-crystal X-ray diffraction study reveals **3** to be remarkably a monomeric structure (vide infra).

(30) (a) Rodriguez-Delgado, A.; Mariott, W. R.; Chen, E. Y.-X. *Macromolecules* **2004**, *37*, 3092−3100. (b) Bovey, F. A.; Mirau, P. A. *NMR of Polymers*; Academic Press: San Diego, 1996. (c) Ferguson, R. C.; Ovenall, D. W. *Macromolecules* **1987**, *20*, 1245−1248. (d) Ferguson, R. C.; Ovenall, D. W. *Polym. Prepr. (Am. Chem. Soc. Div. Polym. Chem.)* **1985**, *26*, 182−183. (e) Subramanian, R.; Allen, R. D.; McGrath, J. E.; Ward, T. C. *Polym. Prepr. (Am. Chem. Soc., Div. Polym. Chem.)* **1985**, *26*, 238−240.

The isolation, characterization, and structure of the ester enolaluminate **3** are of great importance because it simulates the structure of the monomeric active propagating center for the anionic polymerization of (meth)acrylates by the combination of organolithium initiators with organoaluminum compounds.

The $^1$H NMR spectrum of **3** in $C_6D_6$ at 23 °C features sharp, well-resolved peaks for all types of protons present in **3**. Most noticeable are the chemical shifts for the methine proton in $-OCHMe_2$ (3.95 ppm) and the methyl protons in $-OCHMe_2$ (0.78 ppm), which are substantially upfield shifted by 0.33 and 0.46 ppm, respectively, as compared with those of the corresponding signals for the $-OCHMe_2$ (4.28 ppm) and $-OCHMe_2$ (1.24 ppm) protons in the ester enolate complex **2**. These upfield shifts can be explained with the shielding effect imposed by the BHT ligand on the $-OCHMe_2$ group within the structure. In contrast, the Al−Me peak (0.11 ppm) in **3** is downfield shifted by 0.38 ppm from the Al−Me peak in the starting aluminum compound $MeAl(BHT)_2$. Furthermore, the $^{13}$C NMR spectra show that the signal of C(O) [i.e., $=C(O)O^iPr$] shifts upfield from 156.2 ppm in **2** to 150.6 ppm in **3** (by 5.6 ppm) and that the signal of C(α) (i.e., $=CMe_2$) shifts downfield from 78.0 ppm in **2** to 87.6 ppm in **3** (by 9.6 ppm), reflecting the increased double bond character of the C(α) and C(O) bond and also the enhanced covalent character of the metal−oxygen bond in the ester enolaluminate **3**;[15] this also implies that the complexation of the lithium ester enolate with organoaluminum compounds such as $MeAl(BHT)_2$ reduces the nucleophilicity at α-C. Overall, the sharp, well-resolved $^1$H and $^{13}$C NMR resonances and a single, sharp $^6$Li NMR signal at −1.00 ppm (the $^6$Li NMR of EiBLi exhibits two broad peaks at 0.31 and 0.43 ppm[20c]) for complex **3** suggest that its monomeric structure is retained in solution. However, the only observed one type of the BHT ligand in the solution NMR spectra at ambient temperature indicates a fluxional process in which the free and coordinated (to the lithium cation) BHT groups are exchanged rapidly on the NMR time scale.

Thus, the employed $MeAl(BHT)_2$ deaggregates the lithium ester enolate **2** to its monomeric structure and stabilizes it by forming the discrete lithium ester enolaluminate complex **3**. The addition of 2 equiv of $MeAl(BHT)_2$ to **2** also cleanly generates **3** with 1 equiv of $MeAl(BHT)_2$ left unreacted, indicating the excess of $MeAl(BHT)_2$ neither reacts further with nor decomposes **3**. This fact considerably simplifies the activated-monomer polymerization procedures and kinetic experiments, in terms of the ability to readily generate the lithium ester enolaluminate active species (initiator or propagator) and the organoaluminum catalyst by in situ mixing of the lithium enolate **2** with suitable organoaluminum compounds in a predetermined ratio. The formation of the "ate" complex (i.e., the enolaluminate structure) between $^iBu_2Al(BHT)$ and methyl α-lithioisobutylate has been previously observed spectroscopically;[17b] however, we did not observe the formation of the anticipated enolaluminate species from the reactions of **2** with $^iBuAl(BHT)_2$ and $Al(BHT)_3$, presumably due to steric reasons.

To examine whether the presence of the sterically crowded, electron-donating BHT ligand at the aluminum moiety is required or not in terms of stability and isolability of the resulting ester enolaluminate complexes, the bulky aluminum alkyl, $Al(^iBu)_3$, was used to react with **2**. The formation of the desired lithium ester enolaluminate complex, $Li^+[Me_2C{=}C(O^iPr)OAl(^iBu)_3]^-$ (**4**), can be readily identified and characterized based on the spectroscopic characteristics for the enolaluminate moiety (see Experimental Section). However, this product exists as a colorless oil and did not crystallize under various conditions, hampering our structural characterization efforts.

Numerous attempts to isolate the targeted ester enolaluminate complex derived from the reaction of **2** with $Al(C_6F_5)_3$ in nonpolar hydrocarbons, such as toluene, at various temperatures failed to obtain the clean product as it underwent various types of decompositions. However, upon addition of a small amount of donor solvents such as THF, the same reaction in toluene produces the lithium ester enolaluminate complex, $Li^+(THF)_2[Me_2C{=}C(O^iPr)OAl(C_6F_5)_3]^-$ (**5**), which is isolable but thermally unstable. Several attempts to obtain its crystal

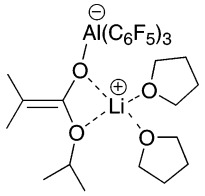


**5**

structure were unsuccessful because of the low quality and thermal instability of the crystals obtained; the proposed structure of **5** shown above is based on the spectroscopic data (see Experimental section) and the structure of **3**. Nevertheless, the formation of the aluminate entity within **5** is evident when comparing its $^{19}$F NMR chemical shifts to those of MMA·$Al(C_6F_5)_3$ (**1**) and our other structurally characterized aluminate complexes having a common structural fragment of $-OAl(C_6F_5)_3^-$.[31] The $^{13}$C NMR spectroscopic data for the enolate moiety are similar to those observed in **3**, with characteristic chemical shifts for the *C*(O) and *C*(α) carbons in **5** being 151.8 and 92.0 ppm, respectively.

Overall, these synthetic studies indicate that the BHT-type ligand within the organoaluminum compound provides the combination of the necessary steric bulkiness and electron-donating ability to deaggregate the lithium ester enolate to its monomer and stabilize it by forming the stable lithium ester enolaluminate. Such aluminum compounds employed, however, can be too bulky to generate the ester enolaluminate species [e.g., $^iBuAl(BHT)_2$ and $Al(BHT)_3$]; the change of the alkyl group from Me in $MeAl(BHT)_2$ to $^i$Bu in $^iBuAl(BHT)_2$ results in a completely different reaction pattern toward the lithium ester enolate and polymerization characteristics (vide infra). For those sterically bulky, non-BHT-carrying organoaluminum compounds such as $Al(^iBu)_3$ and $Al(C_6F_5)_3$, the corresponding enolaluminate complexes can be generated and isolated; however, their structural characterizations were hampered by the noncrystallizability [$Al(^iBu)_3$] or the need to use the external stabilizing reagent [$Al(C_6F_5)_3$].

**Monomer Activation by Organoaluminum Lewis Acids.** Activation of monomer with sterically crowded, strongly Lewis acidic organoaluminum alkyls incorporating bulky phenoxide ligands greatly accelerates the polymerization by aluminum

(31) (a) Bolig, A. D.; Chen, E. Y.-X. *J. Am. Chem. Soc.* **2004**, *126*, 4897−4906. (b) Chakraborty, D.; Chen, E. Y.-X. *Organometallics* **2003**, *22*, 207−210.

***Table 2.*** Selected $^{13}C$ NMR Spectroscopic Data ($C_6D_6$, ppm) for MMA·[Al] Adducts

| adducts | $\delta C$(O) ($\Delta\delta$)[a] | $\delta CH_2$= ($\Delta\delta$)[a] | $\delta CH_3O$ ($\Delta\delta$)[a] |
|---|---|---|---|
| MMA | 167.2 | 124.9 | 51.2 |
| MMA·Al(BHT)$_3$ | 168.1 (+0.9) | 125.0 (+0.1) | 51.1 (−0.1) |
| MMA·Al$^i$Bu$_3$ | 170.9 (+3.7) | 135.0 (+10.1) | 54.0 (+2.8) |
| MMA·Al$^i$Bu(BHT)$_2$ | 171.1 (+3.9) | 136.0 (+11.1) | 54.1 (+2.9) |
| MMA·Al$^i$Bu$_2$(BHT) | 172.7 (+5.5) | 134.5 (+9.6) | 55.6 (+4.4) |
| MMA·AlMe(BHT)$_2$[b] | 174.2 (+7.0) | 136.2 (+11.3) | 57.1 (+5.9) |
| MMA·Al($C_6F_5$)$_3$ | 176.7 (+9.5) | 136.4 (+11.5) | 57.2 (+6.0) |

[a] $\Delta\delta$ relative to MMA. [b] Data taken from ref 33.

porphyrin initiators in Inoue's high-speed living polymerization of methacrylic esters.[32] The activated monomer polymerization mechanism is also believed to be operative in Hatada's stereospecific living methacrylate polymerization by the $^t$BuLi/bulky aluminum phenoxide combination.[6a] Likewise, the activated monomer polymerization mechanism is anticipated for the current polymerization system by the lithium ester enolaluminate (e.g., **3**) in combination with the conjugate bulky aluminum Lewis acid [e.g., MeAl(BHT)$_2$]. To provide the necessary background knowledge for the future discussion on polymerization and mechanism sections, interactions of the monomer, MMA, with six bulky organoaluminum Lewis acids of current interest, including MeAl(BHT)$_2$, $^i$BuAl(BHT)$_2$, $^i$Bu$_2$Al(BHT), Al$^i$Bu$_3$, Al($C_6F_5$)$_3$, and Al(BHT)$_3$, were investigated by way of forming MMA·[Al] adduct complexes from the 1:1 molar ratio reactions and then comparing their $^{13}C$ NMR spectral features; additionally, the molecular structure of the adduct MMA·Al($C_6F_5$)$_3$ (**1**) was also determined by X-ray diffraction.

There are four possible resonance forms (**C**−**F**) associated with the structure of the MMA·[Al] adducts; the relative contribution of each resonance form to the overall structure can be estimated by comparing the relative magnitude of the chemical shift difference ($\Delta\delta$) for each functional group, using MMA as a reference.[33] Based on this argument, the selected

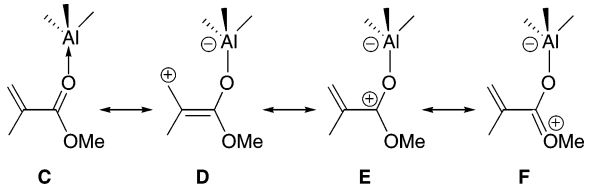


diagnostic $^{13}C$ NMR data for $CH_2$=, $C$(O), $CH_3O$ carbon chemical shifts related to resonance forms **D**, **E**, and **F**, respectively, are compiled in Table 2.

It can be clearly seen from the table that the $^{13}C$ NMR resonances of $C$(O), $CH_2$=, and $CH_3O$ carbons of MMA in the adduct forms are shifted significantly downfield, as compared with those in the free MMA, for all the bulky aluminum Lewis acids investigated, except for the most bulky aluminum phenoxide Al(BHT)$_3$ in the series, which shows minimal to virtually no changes in chemical shifts. This observation implies no activation toward MMA by Al(BHT)$_3$; this inactivity toward the monomer activation correlates well with the observed lack of activity for the MMA polymerization using the combination of **2** and Al(BHT)$_3$ (vide infra). On the other hand, the MMA·Al($C_6F_5$)$_3$ adduct experiences the largest $\Delta\delta$ values for all three types of carbons [i.e., $C$(O), $CH_2$=, and $CH_3O$], arguing for the highest degree of monomer activator by Al($C_6F_5$)$_3$ within this series; this conclusion again correlates well with its observed highest polymerization activity under activated monomer polymerization conditions (vide infra).

For those monomer-activating adducts, the relative magnitude of the $\Delta\delta$ values is, however, different for $C$(O), $CH_2$=, and $CH_3O$ carbons. Consistently for each adduct, the $CH_2$= carbon has the largest $\Delta\delta$ value, followed by $C$(O), whereas the $CH_3O$ carbon is downfield shifted to the least extent. The order of the magnitude of the $\Delta\delta$ values suggests that the relative contribution of each resonance form to the overall structure of all adducts follows this order: **D** > **E** > **F**; this order is an ideal scenario in terms of the activated monomer polymerization, because the resonance structure **D** represents the most active form of the activated monomer toward anionic ester enolaluminate active species in the rate-determining propagating step (vide infra).

**Molecular Structures of Activated Monomer 1, Lithium Ester Enolate Initiator 2, and Lithium Ester Enolaluminate Propagator 3.** Special techniques at low temperatures are required for generation and isolation of suitable single crystals of lithium alkyl ester enolates[11] because of their thermal instability. Owing to this reason, only a handful of lithium ester enolate structures have been reported, but all of which are aggregates (dimer, tetramer, hexamer) either solvated with THF or TMEDA[12] or stabilized by intramolecular Li−N coordination in heteroatom-substituted, lithium α- or β-amino ester enolates.[34] We were not aware of any reported structures of the nondonor-solvated, non-*N*-substituted lithium alkyl ester enolates, although the unsolvated lithium ketone enolates are known.[35] Because the current polymerizations were carried out in toluene, it is of great interest to obtain the crystal structure of the unsolvated lithium ester enolate. Additionally, lithium ester enolaluminate propagating species are structurally unknown; none of such complexes have been previously isolated and structurally characterized. Furthermore, the structures of both the activated monomer and the lithium ester enolaluminate propagator are of importance to the understanding of the fundamental propagating step. Our intense efforts toward these significant fronts have finally yielded X-ray crystal structures of all three key components in the activated-monomer polymerization: activated monomer **1**, initiator **2**, and propagator **3**, shown in Figures 1, 2, and 3, respectively; important bond distances and angles for these three complexes are tabulated in Tables 3−5.

The MMA molecule in complex **1** adopts a s-*cis* conformation as to the C=C and C=O double bonds about the C(19)−C(21) bond and also a s-*cis* conformation as to the C=O and C(20)−O(2) bonds about the C(19)−O(2) bond (Scheme 3). These preferred conformations in the solid-state structure are identical to those observed in the MMA·AlMe$_2$(BHT) adduct[33] and also consistent with the solution conformations for the molecular

(32) (a) Sugimoto, H.; Inoue, S. *Adv. Polym. Sci.* **1999**, *146*, 39−119. (b) Sugimoto, H.; Kuroki, M.; Watanabe, T.; Kawamura, C.; Aida, T.; Inoue, S. *Macromolecules* **1993**, *26*, 3403−3410. (c) Kuroki, M.; Watanabe, T.; Aida, T.; Inoue, S. *J. Am. Chem. Soc.* **1991**, *113*, 5903−5904.
(33) Akakura, M.; Yamamoto, H.; Bott, S.; Barron, A. R. *Polyhedron* **1997**, *16*, 4389−4392.
(34) (a) McNeil, A. J.; Toombes, G. E. S.; Chandramouli, S. V.; Vanasse, B. J.; Ayers, T. A.; O'Brien, M. K.; Lobkovsky, E.; Gruner, S. M.; Marohn, J. A.; Collum, D. B. *J. Am. Chem. Soc.* **2004**, *126*, 5838−5939. (b) Jastrzebski, J. T. B. H.; van Koten, G.; van de Mieroop, W. F. *Inorg. Chim. Acta* **1988**, *142*, 169−171.
(35) (a) Williard, P. G.; Carpenter, G. B. *J. Am. Chem. Soc.* **1986**, *108*, 462−468. (b) Williard, P. G.; Carpenter, G. B. *J. Am. Chem. Soc.* **1985**, *107*, 3345−3346.

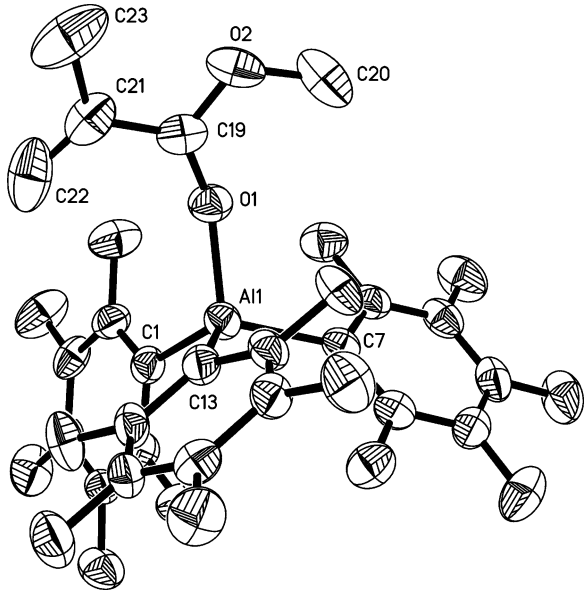


***Figure 1.*** Molecular structure of the activated monomer MMA·Al($C_6F_5$)$_3$ (**1**).

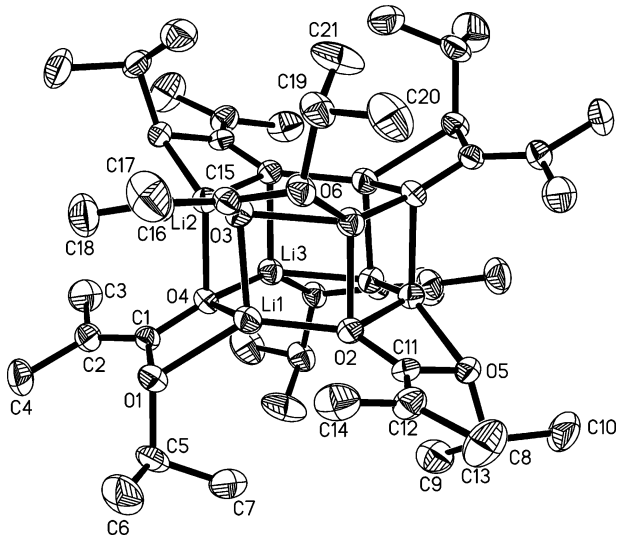


***Figure 2.*** Molecular structure of the initiator [$Me_2C$═C(O$^i$Pr)OLi]$_6$ {[**2**]$_6$}.

complexes between MMA and Lewis acids derived by $^1$H NMR studies.[36] These conformations, however, are different from those found in the crystallographically characterized, *noncoordinated* diphenylmethyl methacrylate[37] and $\eta^2$-C═C coordinated MMA to the Ni{P($C_6H_{11}$)$_3$}$_2$ fragment,[38] both of which adopt s-*trans*, s-*cis* conformations about the C−C and C−O bonds, respectively. As expected, the sum of the angles around both C(19) and C(21) carbons is 360.0° for sp$^2$-hybridized, trigonal-planar carbon centers. When compared with the free diphenylmethyl methacrylate, the activated MMA molecule in complex **1** has nearly the same C═C double bond [1.329(5) Å] length, but shorter internal C−C bond [1.450(5) Å] and C−O bond [1.299(4) Å] lengths by 0.04 Å and a longer C═O bond [1.255(3) Å] length by 0.06 Å. A similar trend is observed when comparing the activated MMA molecular in complex **1** with the free MMA structures (s-*trans* or s-*cis* about the C−C bond) derived from gas electron diffraction studies.[39] The results of these comparative analyses are consistent with the afore-depicted contributions from the resonance forms **D**, **E**, and **F** to the overall structure of the activated MMA molecular **1**.

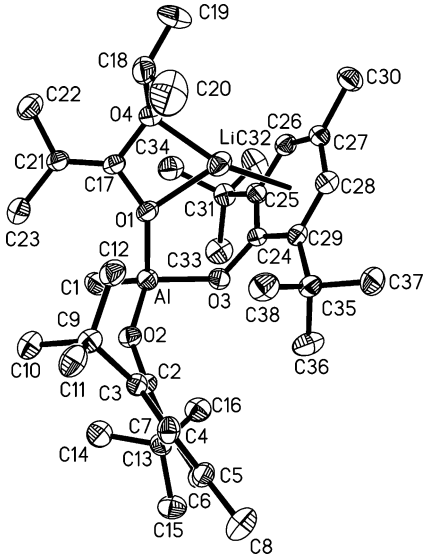


***Figure 3.*** Molecular structure of the propagator Li$^+$[$Me_2$C═C(O$^i$Pr)-OAlMe(BHT)$_2$]$^-$ (**3**).

***Table 3.*** Selected Bond Distances (Å) and Bond Angles (deg) for **1**

| | | | |
|---|---|---|---|
| Al(1)−O(1) | 1.811(2) | Al(1)−C(1) | 1.987(3) |
| Al(1)−C(7) | 1.990(3) | Al(1)−C(13) | 1.993(3) |
| O(1)−C(19) | 1.255(3) | O(2)−C(19) | 1.299(4) |
| O(2)−C(20) | 1.446(4) | C(19)−C(21) | 1.450(5) |
| C(21)−C(22) | 1.329(5) | C(21)−C(23) | 1.483(5) |
| O(1)−Al(1)−C(1) | 108.68(11) | O(1)−Al(1)−C(7) | 107.47(11) |
| O(1)−Al(1)−C(13) | 105.44(12) | C(1)−Al(1)−C(7) | 106.44(12) |
| C(1)−Al(1)−C(13) | 117.31(12) | C(7)−Al(1)−C(13) | 111.12(12) |
| Al(1)−O(1)−C(19) | 148.2(2) | C(19)−O(2)−C(20) | 118.1(3) |
| O(1)−C(19)−O(2) | 118.9(3) | O(1)−C(19)−C(21) | 125.6(3) |
| O(2)−C(19)−C(21) | 115.5(3) | C(22)−C(21)−C(19) | 117.3(3) |
| C(22)−C(21)−C(23) | 125.2(4) | C(19)−C(21)−C(23) | 117.5(4) |

***Table 4.*** Selected Bond Distances (Å) and Bond Angles (deg) for **2**

| | | | |
|---|---|---|---|
| Li(1)−O(2) | 1.862(7) | Li(1)−O(3) | 1.976(7) |
| Li(1)−O(4) | 1.983(7) | Li(1)−O(1) | 2.039(6) |
| Li(2)−O(3) | 1.860(6) | Li(2)−O(4) | 1.971(6) |
| Li(2)−O(2)#1 | 1.979(6) | Li(2)−O(5)#1 | 2.057(6) |
| Li(3)−O(4) | 1.864(6) | Li(3)−O(2)#1 | 1.971(6) |
| Li(3)−O(3)#1 | 1.980(6) | Li(3)−O(6)#1 | 2.059(6) |
| C(1)−O(1) | 1.422(4) | C(1)−O(4) | 1.327(4) |
| C(1)−C(2) | 1.325(5) | C(11)−O(2) | 1.327(4) |
| C(11)−O(5) | 1.412(4) | C(11)−C(12) | 1.322(4) |
| C(15)−O(3) | 1.320(4) | C(15)−O(6) | 1.421(4) |
| C(15)−C(16) | | | 1.322(5) |
| O(1)−Li(1)−O(2) | 142.8(4) | O(1)−Li(1)−O(3) | 118.2(3) |
| O(1)−Li(1)−O(4) | 68.0(2) | O(2)−Li(1)−O(3) | 97.7(3) |
| O(2)−Li(1)−O(4) | 122.5(3) | O(3)−Li(1)−O(4) | 93.4(3) |
| Li(1)−O(4)−Li(3) | 114.2(3) | O(1)−C(1)−O(4) | 109.7(3) |
| O(1)−C(1)−C(2) | 121.4(3) | C(2)−C(1)−O(4) | 128.5(4) |
| C(1)−C(2)−C(3) | 120.3(4) | C(1)−C(2)−C(4) | 123.7(4) |
| C(3)−C(2)−C(4) | | | 116.0(4) |

(36) (a) Furukawa, J.; Kobayashi, E.; Nagata, S. *J. Polym. Sci., Polym. Chem. Ed.* **1976**, *13*, 237−255. (b) Allen, P. E. M.; Bateup, B. O. *Eur. Polym. J.* **1973**, *9*, 1283−1288.
(37) Kageyama, H.; Miki, K.; Tanaka, N.; Kasai, N.; Okamoto, Y.; Hatada, K. Yuki, H. *Makromol. Chem.* **1982**, *183*, 2863−2870.
(38) Jarvis, A. P.; Haddleton, D. M.; Segal, J. A.; McCamley, A. *J. Chem. Soc., Dalton Trans.* **1995**, 2033−2040.
(39) Tsuji, T.; Ito, H.; Takeuchi, H.; Konaka, S. *J. Mol. Struct.* **1999**, *475*, 55−63.

***Scheme 3***

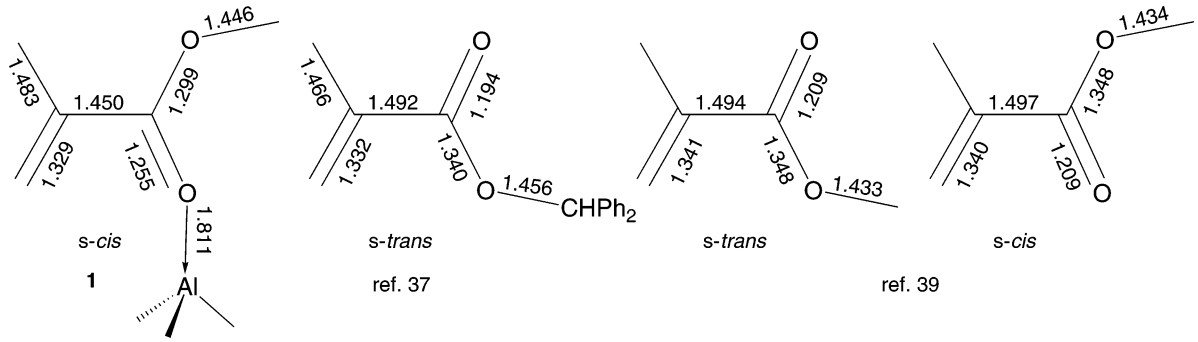


***Table 5.*** Selected Bond Distances (Å) and Bond Angles (deg) for **3**

| | | | |
|---|---|---|---|
| Li−O(1) | 2.002(9) | Li−O(4) | 1.954(8) |
| Li−C(24) | 2.256(8) | Li−C(25) | 2.417(9) |
| Li−C(29) | 2.456(8) | Li−C(26) | 2.488(9) |
| Li−C(28) | 2.536(9) | Li−C(27) | 2.547(9) |
| Al−O(2) | 1.734(3) | Al−O(3) | 1.779(3) |
| Al−O(1) | 1.820(3) | Al−C(1) | 1.955(5) |
| C(17)−O(1) | 1.343(5) | C(17)−O(4) | 1.416(5) |
| C(17)−C(21) | 1.325(6) | C(24)−O(3) | 1.357(5) |
| O(1)−Li−O(4) | 68.5(3) | Al(−O(3)−C(24) | 128.7(3) |
| O(2)−Al−O(3) | 112.63(15) | O(2)−Al−O(1) | 111.14(15) |
| O(3)−Al−O(1) | 96.66(15) | O(2)−Al−C(1) | 105.96(18) |
| O(3)−Al−C(1) | 115.31(18) | O(1)−Al−C(1) | 115.21(18) |
| O(1)−C(17)−O(4) | 107.7(4) | O(1)−C(17)−C(21) | 129.7(4) |
| O(4)−C(17)−C(21) | 122.6(4) | C(17)−C(21)−C(22) | 122.1(4) |
| C(17)−C(21)−C(23) | 121.7(4) | C(22)−C(21)−C(23) | 116.2(4) |

The Al−O distance [1.811(2) Å] in adduct **1** is noticeably shorter than that in the MMA·$AlMe_2$(BHT) adduct [1.867(8) Å], whereas the Al−O−C vector angle [148.2(2)°] is ∼12.5° smaller than that in the MMA·$AlMe_2$(BHT) adduct, indicative of a stronger Al−O $\sigma$ bond in **1**. The geometry around aluminum is a distorted tetrahedron with a sum of the C−Al−C angles of 334.9°, and the average Al−C(aryl) distance (1.990 Å) compares well to those in other $Al(C_6F_5)_3$ complexes with metallocene alkyl,[40] imidazole,[41] toluene,[42] THF,[43] water,[31b] and methanol.[31b]

The lithium ester enolate **2** crystallizes in hexanes as a hexamer (Figure 2), but only half of it is unique and present in the asymmetric unit due to a crystallographically imposed inversion center; this situation resembles the structure of the unsolvated lithium pinacolone enolate.[35] The $Li_6O_6$ core can be described as a hexagonal prism with the hexagonal face defined by alternate Li and O atoms and the edges by Li−O bonds; such a hexameric aggregated structure of prismatic type for methyl α-lithioisobutyrate in nonpolar solvents was also predicted by DFT calculations.[13b] The $Li_3O_3$ hexagonal faces are slightly twisted out of planarity with the maximum deviation being <0.08 Å. The hexagonal $Li_3O_3$ ring is distored, with the average intraring angle at Li (123.5°) being somewhat larger than that at O (116.2°).

Because the metric parameters for the three independent ester enolate anions present in the crystallographic asymmetric unit of **2** are very similar, Scheme 4 depicts only one of three enolates with bond lengths, which is discussed herein. As can be seen from Scheme 4, each of the anionic enolate oxygen

***Scheme 4***

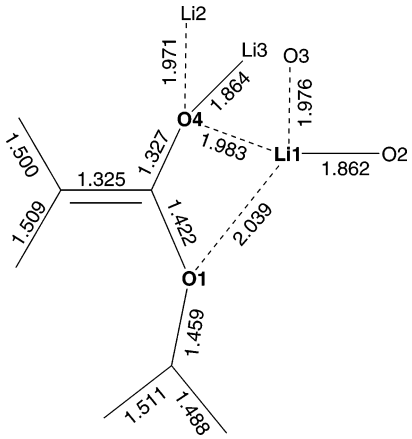


atoms is bonded to three lithium atoms, but each Li is tetrahedrally coordinated to four O atoms because of additional coordination of Li to the alkoxy O atom; this latter coordination mode differs from the previously determined lithium ester enolate structures.[12,34] The four Li−O bonds at each Li center have bond lengths ranging from 1.862 to 2.039 Å, with one of the Li−anionic enolate O bonds being the shortest (Li1−O2 or Li3−O4) and the Li−alkoxy O being the longest (Li1−O1). The chelating effect of the ester enolate ligand by way of Li coordination to the two O centers of the same ester enolate anion molecule results in an acute O1−Li1−O4 angle of only 68.0-(2)°, whereas the O1−Li1−O2 angle is strikingly large [142.8(4)°], both substantially deviating from a tetrahedral angle.

The sum of the angles around the C(α) and C(O) carbons in **2** is 360.0° and 359.6°, respectively, for $sp^2$-hybridized, trigonal-planar carbon centers. A bond length of C1−C2 = 1.325(5) Å is nearly identical to that of the C=C double bond observed in the activated MMA molecular in complex **1**, for a typical C=C double bond; this double-bond length is somewhat shorter than that in the TMEDA-solvated dimer [$Me_2C$=C($O^tBu$)OLi·TMEDA]$_2$ [1.348(6) Å].[12] The C1−O4 (anionic enolate O) bond length [1.327(4) Å] is considerably longer than a typical carbonyl C=O bond by ∼0.13 Å, somewhat shorter than that of the unsolvated lithium pinacolone enolate [1.341(5) Å],[35] and longer than that of [$Me_2C$=C($O^tBu$)OLi·TMEDA]$_2$ [1.304(5) Å].[12] All crystallographical data are consistent with the depicted lithium ester enolate structure.

(40) (a) Liu, Z.; Somsook, E.; Landis, C. R. *J. Am. Chem. Soc.* **2001**, *123*, 2915−2916. (b) Chen, E. Y.-X.; Kruper, W. J.; Roof, G.; Wilson, D. R. *J. Am. Chem. Soc.* **2001**, *123*, 745−746.
(41) LaPointe, R. E.; Roof, G. R.; Abboud, K. A.; Klosin, J. *J. Am. Chem. Soc.* **2000**, *122*, 9560−9561.
(42) Hair, G. S.; Cowley, A. H.; Jones, R. A.; McBurnett, B. G.; Voigt, A. *J. Am. Chem. Soc.* **1999**, *121*, 4922−4923.
(43) Belgardt, T.; Storre, J.; Roesky, H. W.; Noltemeyer, M.; Schmidt, H.-G. *Inorg. Chem.* **1995**, *34*, 3821−3822.

***Scheme 5***

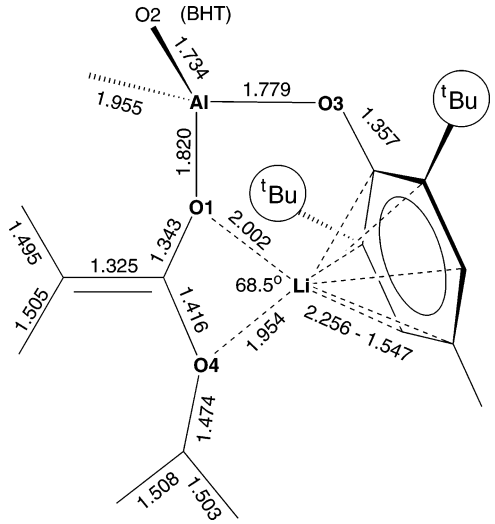


The lithium ester enolaluminate **3** crystallizes in the monoclinic space group $P2_1/n$ from a mixture of toluene and hexanes at −30 °C. The most remarkable structural feature of **3** is its monomeric structure (Figure 3), which can be attributed to stabilization via intramolecular coordination of the lithium cation to both the ester enolate ligand, which serves as a chelating ligand, *and* one of the bulky, electron-donating BHT ligands at Al, which serves as an $\eta^6$-ligand. As can be seen from Scheme 5, the anionic enolate oxygen atom is bonded to both the lithium cation and the aluminum center, whereas the alkoxy O atom is coordinated to only the Li atom. In addition to the coordination to the chelating ester enolate ligand [note again the acute O−Li−O angle of only 68.5(3)°], the Li cation is also coordinated to one of the BHT ligands in an $\eta^6$-fashion. The Li−C bond length, however, spans a wide range, with the Li−C(*ipso*) bond being the shortest [2.256(8) Å], the Li−C(*para*) bond the longest [2.547(9) Å], and the Li−C(*ortho*) and Li−C(*meta*) bonds between [from to 2.417(9) Å to 2.536(9) Å]. Using a working criterion for coordination to the metal cations that the metal−atom distance not be greater than the sum of the van der Waals radii of the metal and atom as listed by Pauling, the mean Li−C length is 2.259 Å, with minimum and maximum Li−C lengths being 2.041 and 2.557 Å, respectively.[44] Hence, the observed distances between Li and the BHT-ring carbons are within the defined bonding range.

The C═C double bond length in **3** is identical to that in **2**, and other metric parameters associated with the ester enolate moiety are remarkably similar to those observed in **2** as well, except for a somewhat lengthened C−O1 (enolate anion O) bond and shortened C−O4 (alkoxy O) bond in **3**. The geometry around the four-coordinate aluminum center is that of a distorted tetrahedron with a sum of the O−Al−O angles of 320.4°. The Al−C bond in **3** [1.955(5) Å] is somewhat longer than that found in the neutral $MeAl(BHT)_2$ [1.927(3) Å],[24] as predicted on changing from a planar to tetrahedral geometry in terms of the increased p character in the Al−C bond. The Al−O (BHT) bonds in **3** [1.779(3), 1.734(3) Å] are also longer than those found in the neutral $MeAl(BHT)_2$ [1.687(2), 1.685(2) Å].[24] On the other hand, the change in geometry adapted for the $\eta^6$-coordination of one of the BHT ligands to the Li cation results in two striking angles associated with the coordinated BHT ligand: the smallest O1−Al−O3 angle [98.7(2)°] as compared with the rest of the angles at the Al center in **3** and the significantly smaller Al−O3−C(*ipso*) angle [128.7(3)°] for the coordinated BHT ligand than that for the noncoordinated BHT ligand [150.1(3)°] in **3**. The aryl ring in the coordinated BHT ligand is more planar than is the noncoordinated BHT ligand at Al; the maximum deviations of the carbon atoms from planes defined by C24 to C29 and C2 to C7 atoms are <0.083 and <0.12 Å, respectively. To the best of our knowledge, the structure of **3** represents the first example of crystallographically characterized monomeric lithium ester enolates or enolaluminates.

**Polymerization of Methacrylates by Lithium Ester Enolaluminate Active Species.** Table 6 summarizes the results of MMA and BMA polymerizations by the lithium ester enolate **2** and enolaluminate **3** with and without the catalyst, $MeAl(BHT)_2$. As anticipated, the MMA polymerization in toluene by the aggregating initiator **2** produces *isotactic* PMMA {[*mm*] = 75.5%} with a broad MWD (PDI = 6.8) and a low initiator efficiency of $I^* = 43\%$ (run 1, Table 6). In sharp contrast, the enolaluminate **3** produces *syndiotactic* PMMA {[*rr*] = 72.9%} with a much narrower MWD (PDI = 1.20, run 2). The polymer yield, however, is reduced by one-fourth as compared with that by **2**, reflecting the lower reactivity of lithium enolaluminates vs lithium enolates as previously alluded to on the basis of the spectroscopic data. In the presence of 1 equiv of the conjugate Lewis acid catalyst $MeAl(BHT)_2$, the polymerization by **3** becomes highly active, producing PMMA in quantitative yield and with a low PDI value of 1.12 (run 3), providing evidence for the activated-monomer polymerization. As discussed earlier, the second equivalent of $MeAl(BHT)_2$ does not further react with **3** but forms the stable activated monomer−aluminum complex. Lowering the polymerization temperature to 0 °C increases the syndiotacticity to 79.3% and the initiator efficiency to 81%, but the PDI value is kept the same (run 4 vs 3). Further lowering of the polymerization temperature to −40 °C quadruples the time for achieving a quantitative polymer yield; however, four other important polymer and polymerization characteristics, including $M_n$, PDI, $I^*$, and [*rr*], are virtually unaffected (run 5 vs 4), indicating the controlled behavior of this polymerization over a broad temperature range.

The BMA polymerization by the propagator/catalyst pair, **3**/$MeAl(BHT)_2$, is as effective as the MMA polymerization, producing PBMA with a narrow MWD and moderately high syndiotacticity of 86.6% (run 6). The PBMA-*b*-PMMA block copolymer with a narrow MWD (PDI = 1.12) has also been synthesized with virtually a quantitative initiator efficiency (run 7); the molar composition of two monomer units in the block copolymer obtained from the $^1H$ NMR analysis is the same as the monomer molar feed ratio (i.e., 1:1), and the syndiotacticity of the block copolymer is collectively ∼84%, an overall value accounting for both blocks.[30a] Thus, several lines of evidence, including the observed narrow MWD (PDI < 1.18) of PMMA and PBMA formed, the production of the well-defined block copolymer, and the observed linear increase of the polymer $M_n$ vs polymer yield, which is coupled with the small, nearly constant PDI values (Figure 4), suggest living characteristics of the **3**/$MeAl(BHT)_2$ system.

(44) (a) Williard, P. G. *Comprehensive Organic Synthesis*; Pergamon: New York, 1991; Vol. 1, pp 1−47. (b) Setzer, W. H.; Schleyer, P. V. R. *Adv. Organomet. Chem.* **1985**, *24*, 353−451.

***Table 6.*** MMA and BMA Polymerization Results by Lithium Enolate **2** and Enolaluminate **3**[a]

| run no. | initiator/catalyst/ monomer | $T_p$ (°C) | $t_p$ (h) | yield (%) | $10^4\ M_n$[b] (g/mol) | PDI[b] ($M_w/M_n$) | $I^*$[c] (%) | [*rr*][d] (%) | [*mr*][d] (%) | [*mm*][d] (%) |
|---|---|---|---|---|---|---|---|---|---|---|
| 1 | **2**/MMA | 23 | 1 | 80 | 3.75 | 6.8 | 43 | 8.1 | 16.4 | 75.5 |
| 2 | **3**/MMA | 23 | 1 | 22 | 2.24 | 1.20 | 20 | 72.9 | 24.6 | 2.5 |
| 3 | **3**/MeAl(BHT)$_2$/MMA | 23 | 1 | >99 | 3.21 | 1.12 | 62 | 71.3 | 24.7 | 4.0 |
| 4 | **3**/MeAl(BHT)$_2$/MMA | 0 | 1 | >99 | 2.46 | 1.12 | 81 | 79.3 | 19.9 | 0.8 |
| 5 | **3**/MeAl(BHT)$_2$/MMA | −40 | 4 | >99 | 2.45 | 1.09 | 82 | 79.5 | 19.6 | 0.9 |
| 6 | **3**/MeAl(BHT)$_2$/ BMA | 0 | 1 | >99 | 3.38 | 1.18 | 84 | 86.7 | 12.6 | 0.7 |
| 7 | **3**/MeAl(BHT)$_2$/ BMA/MMA | 0 | 1/1 | >99 | 4.69 | 1.12 | 102 | 83.6 | 16.4 | 0.0 |

[a] $[Monomer]_0/[initiator]_0 = 200$, 5 mL of toluene. [b] Number-average molecular weight ($M_n$) and polydispersity index (PDI) determined by GPC relative to PMMA standards. [c] Initiator efficiency ($I^* = M_n(calcd)/M_n(exptl)$). [d] Tacticity (methyl triad distributions) determined by $^1H$ NMR spectroscopy in $CDCl_3$.

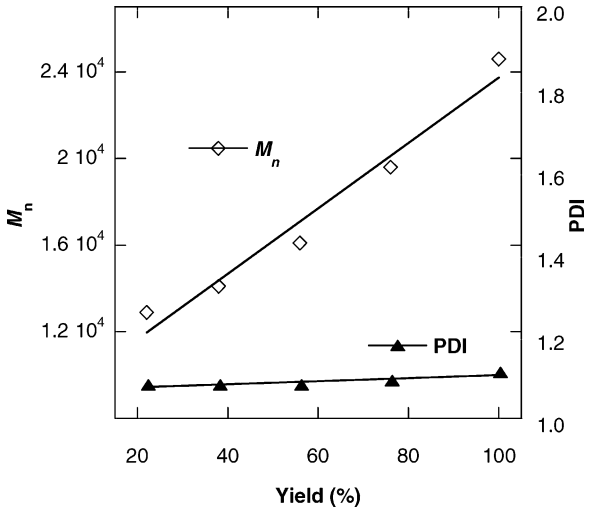


***Figure 4.*** Plot of $M_n$ and PDI of PMMA by **3**/MeAl(BHT)$_2$ at 0 °C vs polymer yield.

The results from the investigation of structural effects of five additional bulky Lewis acidic aluminum catalysts and the corresponding enolaluminates derived from them on the behavior of MMA polymerization are summarized in Table 7. The lithium enolaluminate generated from **2** and Al($^i$Bu)$_3$ produces essentially atactic PMMA with relatively large PDI values of >1.3 (runs 1 and 2, Table 7). Consistent with the activated-monomer polymerization, when using 2 equiv of Al($^i$Bu)$_3$ vs **2** (to form a 1/1 ratio of enolaluminate/catalyst, vide supra), the same polymerization becomes not only syndioselective but also well-behaved with PDI < 1.17 (runs 3 and 4). A gradual increase of the steric bulkiness of the organoaluminum compounds by sequential substitution of the $^i$Bu ligand with the BHT ligand results in *pronounced* changes in the MMA polymerization behavior. Thus, as compared with Al($^i$Bu)$_3$, the polymerization using $^i$Bu$_2$Al(BHT) is noticeably more syndioselective (runs 5−7 vs 1−4); the syndioselectivity of the MMA polymerization by the sterically bulkier $^i$BuAl(BHT)$_2$ is further enhanced, but with substantially reduced activity and an even bimodal MWD (runs 8−10). Most strikingly, the polymerization is shut down with the sterically bulkiest Al(BHT)$_3$ in this series (runs 11−13). The small amount of PMMA formed from a run with an extended polymerization time shows to be isotactic (run 13), indicative of the polymer formed by the lithium enolate alone[17] (i.e., no participation of the activated monomer or the lithium enolaluminate); this observation is consistent with the previously discussed finding of no activation of MMA by Al(BHT)$_3$ and no enolaluminate formation when mixing **2** and Al(BHT)$_3$. In the case of $^i$BuAl(BHT)$_2$, considerable monomer activation, at least to the same level as that by Al($^i$Bu)$_3$, has been observed (vide supra); however, it is its inability to form the observable enolaluminate propagating species that renders its ill-behaved polymerization with only marginal activity. In agreement with the finding of the related systems investigated by Holmes and co-workers,[17] the results obtained from the current system show that, to achieve a high degree of polymerization control and the syndiotacticity of polymer, organoaluminum compounds must have the structures capable of forming both monomeric ester enolaluminate and activated-monomer complexes.

The alane, Al($C_6F_5$)$_3$, is a unique activator or catalyst because the three $C_6F_5$ groups provide both adequate steric protection of the aluminum center, rendering its monomeric form,[42] and high electron-withdrawing capacity, rendering its remarkably high Lewis acidity.[40b] Thus, it is of great interest to use this alane, in combination with the initiator **2**, for MMA polymerization. While the 1:1 mixture of **2** and Al($C_6F_5$)$_3$ (to generate the enolaluminate in situ) at 23 °C is inactive, the polymerization using a 1:2 ratio (to generate both the enolaluminate propagator and the activated monomer) is highly active, producing syndiotactic {[*rr*] = 73.5%} PMMA with quantitative yield and a narrow MWD (PDI = 1.14, run 15, Table 7). When the same polymerization is carried out at 0 °C, syndiotactic {[*rr*] = 82.5%} PMMA with PDI as small as 1.04 is obtained (run 16). The instability of the enolaluminate derived from Al($C_6F_5$)$_3$ in nonpolar solvents (vide supra) presumably causes the observed much-higher-than-calculated $M_n$ (i.e., low $I^*$ values); however, this problem can be largely overcome by changing the reagent addition sequence in the polymerization procedures as we have demonstrated that such an enolaluminate is stable in donor solvents. Hence, instead of preforming the enolaluminate by premixing **2** and Al($C_6F_5$)$_3$ in toluene, the addition of an alane solution in toluene to MMA, followed by addition of **2** to start the polymerization, allowed for a drastically increased initiator efficiency ($I^*$ = 72%) but the same narrow MWD (PDI = 1.04, run 17).

**Polymerization Kinetics and Mechanism.** Scheme 6 illustrates the proposed bimolecular chain propagation for the MMA polymerization by the lithium ester enolaluminate and organoaluminum catalyst combination. This mechanism involves Michael addition of enolaluminate propagator **G** to Al-activated monomer **H**, followed by the release of the coordinated aluminum catalyst to the ester group of the polymer chain by MMA to regenerate the propagating species **G** and the activated

***Table 7.*** Effect of Enolaluminate and Aluminum Catalyst Structures on MMA Polymerization[a]

| run no. | initiator/ activator | $T_p$ (°C) | $t_p$ (h) | yield (%) | $10^4\ M_n$[b] (g/mol) | PDI[b] ($M_w/M_n$) | [*rr*][c] (%) | [*mr*][c] (%) | [*mm*][c] (%) |
|---|---|---|---|---|---|---|---|---|---|
| 1 | **2**/Al($^i$Bu)$_3$ | 23 | 1 | 40 | 3.49 | 1.32 | 27.6 | 47.6 | 24.8 |
| 2 | **2**/Al($^i$Bu)$_3$ | 0 | 4 | >99 | 1.76 | 1.31 | 37.2 | 42.0 | 20.8 |
| 3 | **2**/2Al($^i$Bu)$_3$ | 23 | 1 | >99 | 3.24 | 1.08 | 57.8 | 35.2 | 7.0 |
| 4 | **2**/2Al($^i$Bu)$_3$ | 0 | 4 | >99 | 2.83 | 1.17 | 63.0 | 32.9 | 4.1 |
| 5 | **2**/Al($^i$Bu)$_2$(BHT) | 23 | 1 | 22 | 1.49 | 1.16 | 49.0 | 38.3 | 12.7 |
| 6 | **2**/2Al($^i$Bu)$_2$(BHT) | 23 | 1 | 89 | 3.38 | 1.51 | 64.5 | 31.8 | 3.7 |
| 7 | **2**/2Al($^i$Bu)$_2$(BHT) | 0 | 4 | >99 | 3.71 | 1.16 | 69.0 | 27.4 | 3.7 |
| 8 | **2**/Al($^i$Bu)(BHT)$_2$ | 23 | 1 | 4 | | | | | |
| 9 | **2**/2Al($^i$Bu)(BHT)$_2$ | 23 | 1 | 6 | | | 72.7 | 23.0 | 4.3 |
| 10 | **2**/2Al($^i$Bu)(BHT)$_2$ | 0 | 4 | 12 | 11, 0.8 | 2.9, 1.1 | 75.4 | 20.0 | 4.6 |
| 11 | **2**/Al(BHT)$_3$ | 23 | 1 | trace | | | | | |
| 12 | **2**/2Al(BHT)$_3$ | 23 | 1 | trace | | | | | |
| 13 | **2**/2Al(BHT)$_3$ | 23 | 4 | 5 | | | 9.5 | 25.7 | 64.8 |
| 14 | **2**/Al(C$_6$F$_5$)$_3$ | 23 | 1 | trace | | | | | |
| 15 | **2**/2Al(C$_6$F$_5$)$_3$ | 23 | 1 | >99 | 11.9 | 1.14 | 73.5 | 24.6 | 1.9 |
| 16 | **2**/2Al(C$_6$F$_5$)$_3$ | 0 | 0.5 | >99 | 11.0 | 1.04 | 82.5 | 15.9 | 1.6 |
| 17[d] | **2**/2Al(C$_6$F$_5$)$_3$ | 0 | 1 | >99 | 6.92 | 1.04 | 79.6 | 19.4 | 1.0 |

[a] $[MMA]_0/[\mathbf{2}]_0 = 200$, 5 mL of toluene. [b] Number-average molecular weight ($M_n$) and polydispersity index (PDI) determined by GPC relative to PMMA standards. [c] Tacticity (methyl triad distributions) determined by $^1$H NMR spectroscopy in $CDCl_3$. [d] Conditions: $[MMA]_0/[\mathbf{2}]_0 = 500$, 10 mL of toluene. Addition sequence: Al(C$_6$F$_5$)$_3$ in toluene, MMA, and **2**.

***Scheme 6***

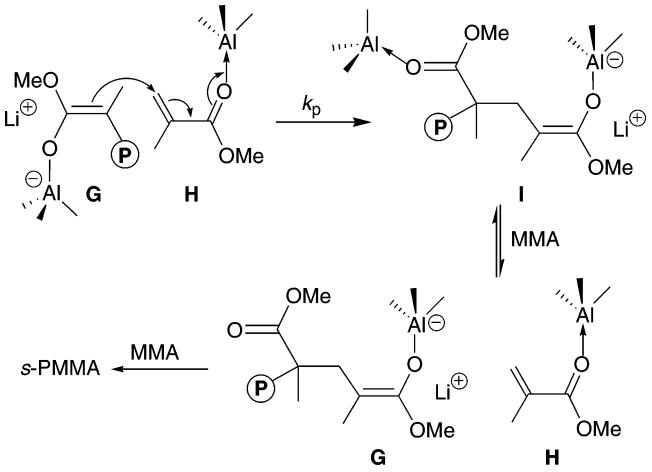


monomer **H**; repeated Michael additions of **G** to **H** produce the polymer in a controlled fashion.

If the release of the catalyst from the ester group of the polymer to the incoming monomer (i.e., **I** + MMA → **G** + **H**) is fast relative to the addition step (i.e., **G** + **H** → **I**) and the equilibrium favors the formation of activated monomer **H**, application of the steady-state approximation of the intermediate **I** results in first-order kinetics with respect to active species [**G**] (i.e., the enolaluminate propagator concentration [Al$^-$]) and activated monomer [**H**] (i.e., the aluminum catalyst concentration [Al]$_0$) but zero-order kinetics in monomer concentration [M]:

$$-\frac{d[M]}{dt} = k_p[\mathbf{G}][\mathbf{H}] = k_p[Al^-][Al]_0 \qquad (1)$$

$$\frac{[M]_0 - [M]_t}{[M]_0} = x_p(\text{conversion}) = k_{app}t \qquad (2)$$

This type of polymerization kinetics has been observed for the MMA polymerizations by the nonbridged zirconocene enolate/zirconocenium cation[45] and enamine/Lewis acid[46] combinations.

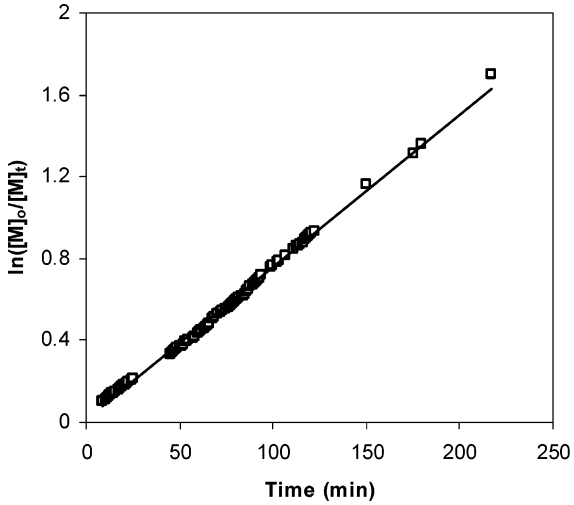


***Figure 5.*** First-order time-conversion plot of the MMA polymerization in toluene-$d_8$ at 22 °C. Conditions: $[MMA]_0 = 1.0$ M, $[\mathbf{3}]_0 = 5.0$ mM, [MeAl(BHT)$_2$]$_0$ = 5.0 mM.

The monitoring of the polymerization by the enolaluminate/organoaluminum combination [i.e., the **3**/MeAl(BHT)$_2$ pair] using the NMR techniques clearly shows, however, the first-order dependence of monomer concentration (Figure 5); this implies that coordination of the aluminum catalyst to the ester group of the polymer chain and to the monomer is competitive:

$$\mathbf{I} + \text{MMA} \overset{K}{\rightleftharpoons} \mathbf{G} + \mathbf{H} \qquad (3)$$

Schlaad and Müller showed that the equilibrium constants for complexation of Al($^i$Bu)$_3$ with MMA and methyl pivalate (serving as a model for the ester group of the polymer chain) are approximately the same,[15] giving for eq 3 $K \approx 1$. Because of this coordination competing process, the concentration of the activated monomer [**H**] now depends on monomer conversion:

(45) (a) Bandermann, F.; Ferenz, M.; Sustmann, R.; Sicking, W. *Macromol. Symp.* **2001**, *174*, 247−253. (b) Li, Y.; Ward, D. G.; Reddy, S. S.; Collins, S. *Macromolecules* **1997**, *30*, 1875−1883.

(46) Miyamoto M.; Kanetaka, S.-Y. *J. Polym. Sci., Part A: Polym. Chem.* **1999**, *37*, 3671−3679.

$$[\mathbf{H}] = (1 - x_p)[\mathbf{H}]_o = \frac{[M]_t}{[M]_0}[Al]_0 \quad (4)$$

Assuming that $MeAl(BHT)_2$ behaves similarly to $Al(^iBu)_3$ in terms of complexation with MMA and the ester group of the polymer and using a rate expression worked out by Schlaad and Müller,[15a] we have a first-order dependence:

$$-\frac{d[M]}{dt} = k_p[\mathbf{G}][\mathbf{H}] = k_p[Al^-]\left(\frac{[M]_t}{[M]_0}[Al]_0\right) \quad (5)$$

$$\ln\frac{[M]_0}{[M]_t} = \left(\frac{k_p[Al^-][Al]_0}{[M]_0}\right)t = k_{app}t \quad (6)$$

Hence, the polymerization should follow first-order kinetics with respect to the active species, aluminum catalyst, and monomer concentrations. To investigate the rate order of the aluminum catalyst in the current MMA polymerization by the **3**/$MeAl(BHT)_2$ pair, polymerization kinetics with varied concentrations of $MeAl(BHT)_2$ at a constant concentration of **3** were carried out in stirred glass reactors. In each $[MeAl(BHT)_2]_0$ (note that this is the concentration of the "free" aluminum catalyst after the formation of **3**), first-order kinetics in [MMA] were observed up to high monomer conversions (≥90%), Figure 6. A double logarithm plot (Figure 7) of the apparent rate constants ($k_{app}$), which were obtained from the slopes of the best-fit lines to the plots of $\ln([M]_0/[M]_t)$ versus time, as a function of $[MeAl(BHT)_2]_0$ was fit to a straight line of slope = 1.1(1). This rate order of 1.1(1) in $[MeAl(BHT)_2]_0$ is the same as that obtained by the in situ monitoring of the polymerization using NMR techniques, although the polymerizations in the NMR tubes were considerably slower (due to the lack of stirring) than those carried out in the stirred reactors. These results indicate that the rate order in $[MeAl(BHT)_2]_0$ is approximately unity, and this polymerization can be described as the activated-monomer polymerization.

The syndiotacticity of the resulting polymers produced via the activated monomer propagation can be understood from Scheme 7, which shows the propagating step of methacrylate polymerization involving the Michael addition of the enolaluminate active species to the activated monomer in the s-*cis* conformation; for steric considerations, ester groups of the monomer and the last added monomer unit are placed on the opposite side, and the resulting polymer linkage is syndiotactic. Noteworthy is the observed, nearly constant syndiotacticity {[*rr*] ≈ 75%} for the MMA polymerizations at all the $[MeAl(BHT)_2]_0$/[**3**] ratios (1, 2, 3, and 4) and at all conversions, indicating the activated-monomer polymerization occurs throughout the course of the polymerization. It should be reminded that the combined spectroscopic and polymerization studies concluded that lithium ester enolaluminates are less reactive than lithium ester enolates. For example, the enolaluminate species, either isolated or generated in situ, have low or no activity toward MMA polymerization. However, under the activated-monomer polymerization conditions (i.e., in the presence of the conjugate aluminum catalysts), these less reactive enolaluminate propagating species become selective and preferentially add to the activated monomer. Therefore, both formations of the enolaluminate and the activated monomer complex are necessary for achieving syndiotacticity and polymerization control.

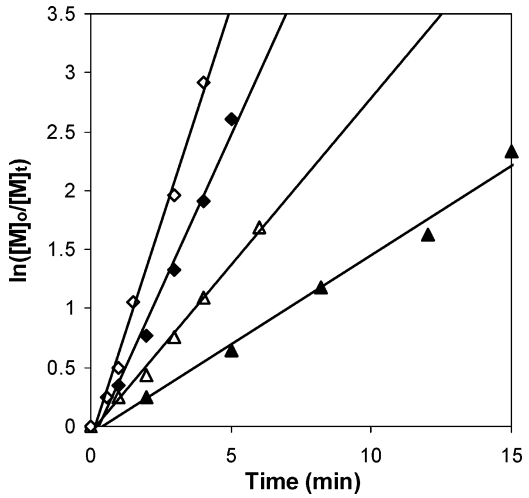


***Figure 6.*** Semilogarithmic plots of $\ln\{[M]_0/[M]_t\}$ versus time for the polymerization of MMA by **3** and $MeAl(BHT)_2$ in toluene at 23 °C. Conditions: $[MMA]_0 = 1.87$ M, $[\mathbf{3}]_0 = 9.34$ mM, $[MeAl(BHT)_2]_0 = 9.34$ mM (▲), 18.7 mM (△); 28.0 mM (◆), 37.4 mM (◇).

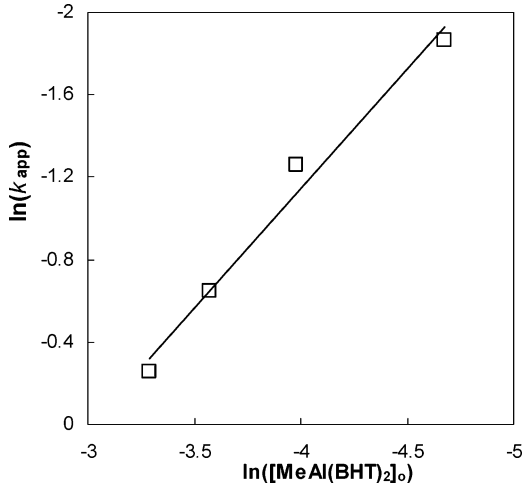


***Figure 7.*** Plot of $\ln(k_{app})$ versus $\ln\{[MeAl(BHT)_2]_0\}$ for the MMA polymerization by **3** and $MeAl(BHT)_2$ in toluene at 23 °C.

***Scheme 7***

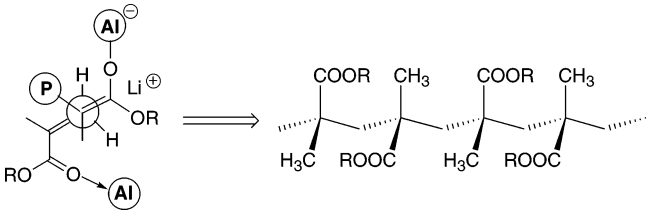


## Summary

In conclusion, the combined synthetic, structural, polymerization, and kinetic study has established the monomeric lithium ester enolaluminate as the single-site anionic propagating center and the bimolecular, activated-monomer mechanism for the controlled polymerization of methacrylates in the presence of conjugate Lewis acidic, bulky organoaluminum catalysts. With suitable structures, the organoaluminum compounds function as deaggregating and stabilizing agents for lithium ester enolates by forming the stable, monomeric ester enolaluminate active species and as catalysts for monomer activation, when used in excess for methacrylate polymerization; these attributes account for the often-observed controlled polymerization by the com-

bination of lithium ester enolates with organoaluminum compounds. Because of the competitive coordination of the organoaluminum catalyst to the monomer and the ester group of the polymer chain, the activated-monomer polymerization of the present system follows first-order kinetics with respect to both monomer and catalyst concentrations.

The fully characterized monomeric lithium ester enolaluminate **3**, which serves as the structural model for the single-site anionic propagating center, exhibits the unique mode of intramolecular coordination of the lithium cation to both oxygen atoms of the ester enolate moiety, acting as a chelating ligand, and to one of the BHT ligands at the aluminate center in an $\eta^6$-fashion; these structural characteristics account for the isolability and monomeric feature of this complex. The structural variations of the employed organoaluminum compounds have substantial influence on the degree of monomer activation, enolaluminate formation and reactivity, and polymerization control. Ester enolaluminates are less reactive than ester enolates but more selective with preferential addition to the activated monomer in a syndioselective fashion. Hence, to achieve the syndiotacticity of polymer and a high degree of polymerization control, the organoaluminum compounds added to the polymerization initiated by lithium ester enolates are required to have structures capable of forming both monomeric ester enolaluminates and activated-monomer complexes. The results obtained from the current investigation of the single-site anionic polymerization, coupled with the previous findings from other related systems,[5−7,15−17] establish the general guidance for the design and synthesis of more efficient and controlled anionic initiators and catalysts.

**Acknowledgment.** This work was supported by the National Science Foundation and Colorado State University. We thank Susie M. Miller for determination of the crystal structures and Boulder Scientific Co. for the gift of $B(C_6F_5)_3$. E.Y.C. acknowledges an Alfred P. Sloan Research Fellowship.

**Supporting Information Available:** Crystallographic data for **1**, **2**, and **3** (CIF) and representative GPC traces (PDF). This material is available free of charge via the Internet at http://pubs.acs.org.

JA044671Z